Società Italiana Infrastrutture Viarie

XIX International SIIV Summer School , Perugia 4^{th} - 8^{th} September 2023

Transportation Infrastructures towards Green Transition

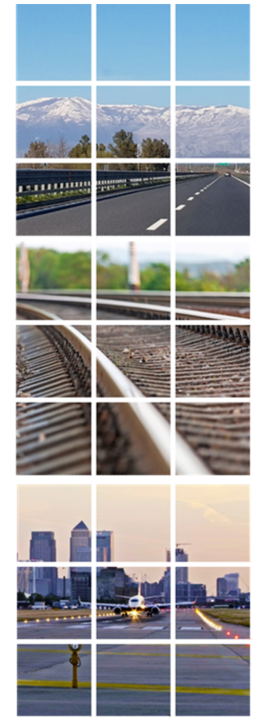

Performance evaluation of sustainable pavement materials by machine learning methods

7 SEPTEMBER .23

Università degli Studi di Perugia
Department of Civil and Environmental Engineering

Nicola Baldo
Polytechnic Department of Engineering and Architecture
University of Udine, Italy

Towards a green and digital future: Twin transitions in the European Union

Ideally Green and Digital transitions <u>reinforce each other</u>!

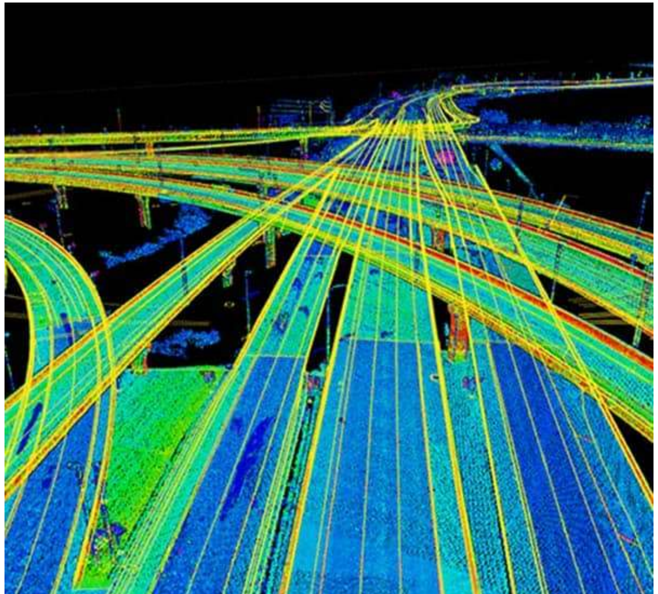

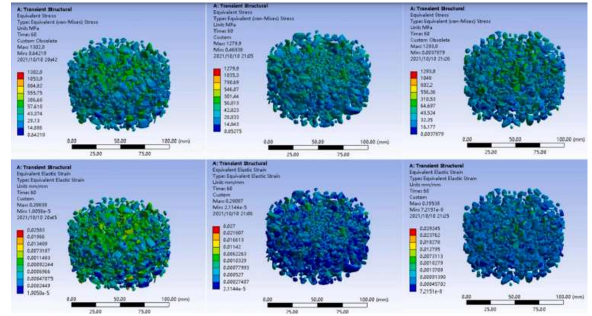

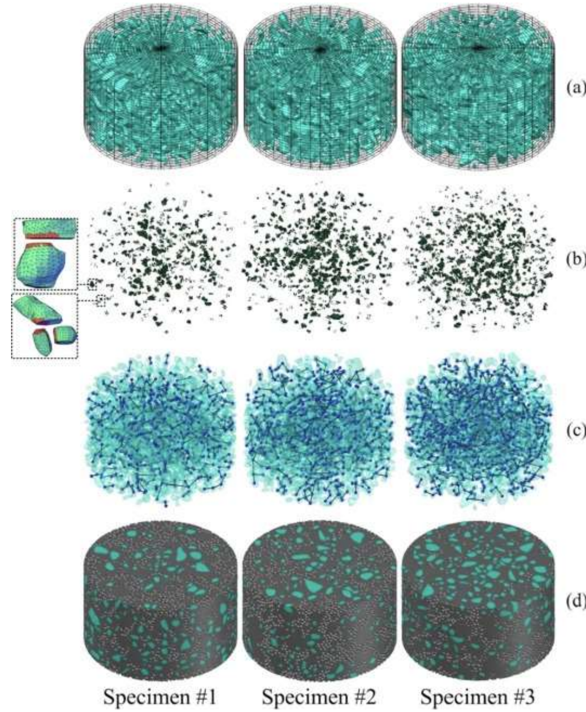
(a)
(b)
(c)
(d)
Specimen #1
Specimen #2
Specimen #3

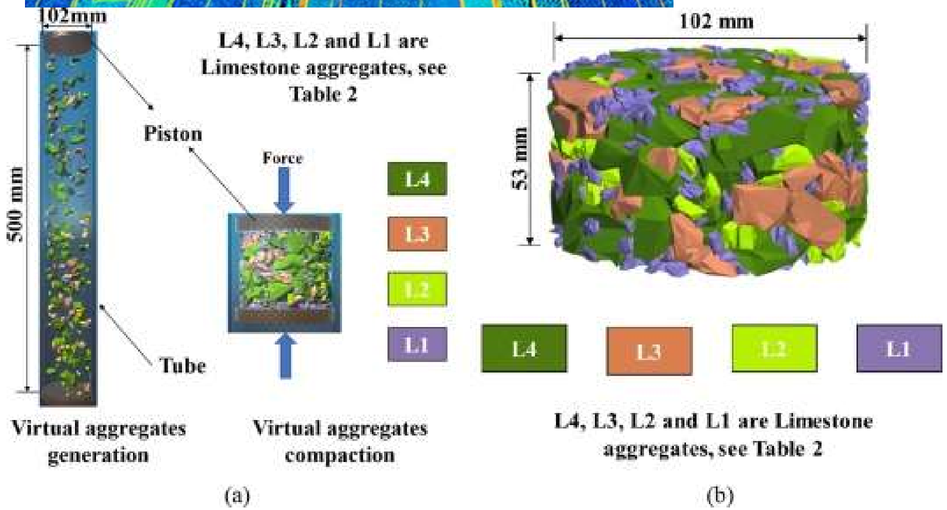
102mm
500 mm
Piston
Tube
L4, L3, L2 and L1 are
Limestone aggregates, see
Table 2
Force
L4
L3
L2
L1
Virtual aggregates
generation
Virtual aggregates
compaction
(a)
102 mm
53 mm
L4
L3
L2
L1
L4, L3, L2 and L1 are Limestone
aggregates, see Table 2
(b)

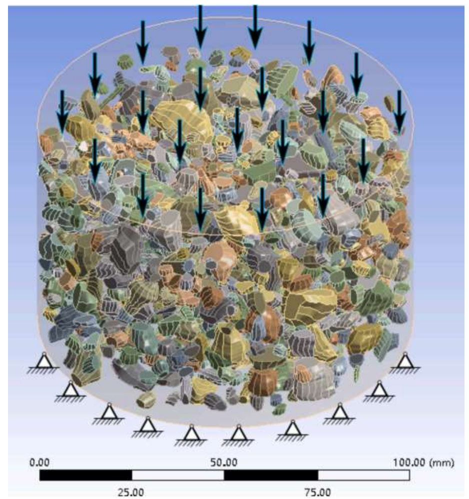
0.00
50.00
100.00 (mm)
25.00
75.00

Road Materials and Pavement Design ›
Latest Articles

Submit an article | Journal homepage

Enter keywords, authors,

133
Views
0
CrossRef
citations to date
0
Altmetric

Research Article

Prediction of Marshall design parameters of asphalt mixtures via machine learning algorithms based on literature data

Mert Atakan & Kürşat Yıldız

Received 21 Nov 2021, Accepted 09 May 2023, Published online: 23 May 2023

ELSEVIER
Construction and Building Materials
Volume 168, 20 April 2018, Pages 660-670

Optimizing asphalt mix design process using artificial neural network and genetic algorithm

Haissam Sebaaly [a], Sudhir Varma [b], James W. Maina [a]

Research | Open Access | Published: 18 March 2022

Prediction of the hot asphalt mix properties using deep neural networks

Kareem Othman

Beni-Suef University Journal of Basic and Applied Sciences **11**, Article number: 40 (2022) | Cite this article

ELSEVIER
Construction and Building Materials
Volume 325, 28 March 2022, 126607

Optimizing asphalt mix design through predicting effective asphalt content and absorbed asphalt content using machine learning

Jian Liu [a], Fangyu Liu [a], Chuanfeng Zheng [b], Daodao Zhou [c], Linbing Wang [a]

Chapter | Jul 18, 2019

International Airfield and Highway Pavements Conference 2019

Artificial Intelligence Based Mix Design of Pavement Mixes

Authors: Rajib B. Mallick, M. K. Nivedya, and Ramkumar Veeraragavan | AUTHOR AFFILIATIONS

Topics of the lecture:

- ✓ **Machine Learning overview**
- ✓ **Case study n.1**
- ✓ **Case study n.2**
- ✓ **Case study n.3**
- ✓ **Case study n.4**
- ✓ **Case study n.5**

Artificial Intelligence vs Machine Learning vs Artificial Neural Networks vs Deep Learning: <u>The Russian Nesting Doll Analogy</u>

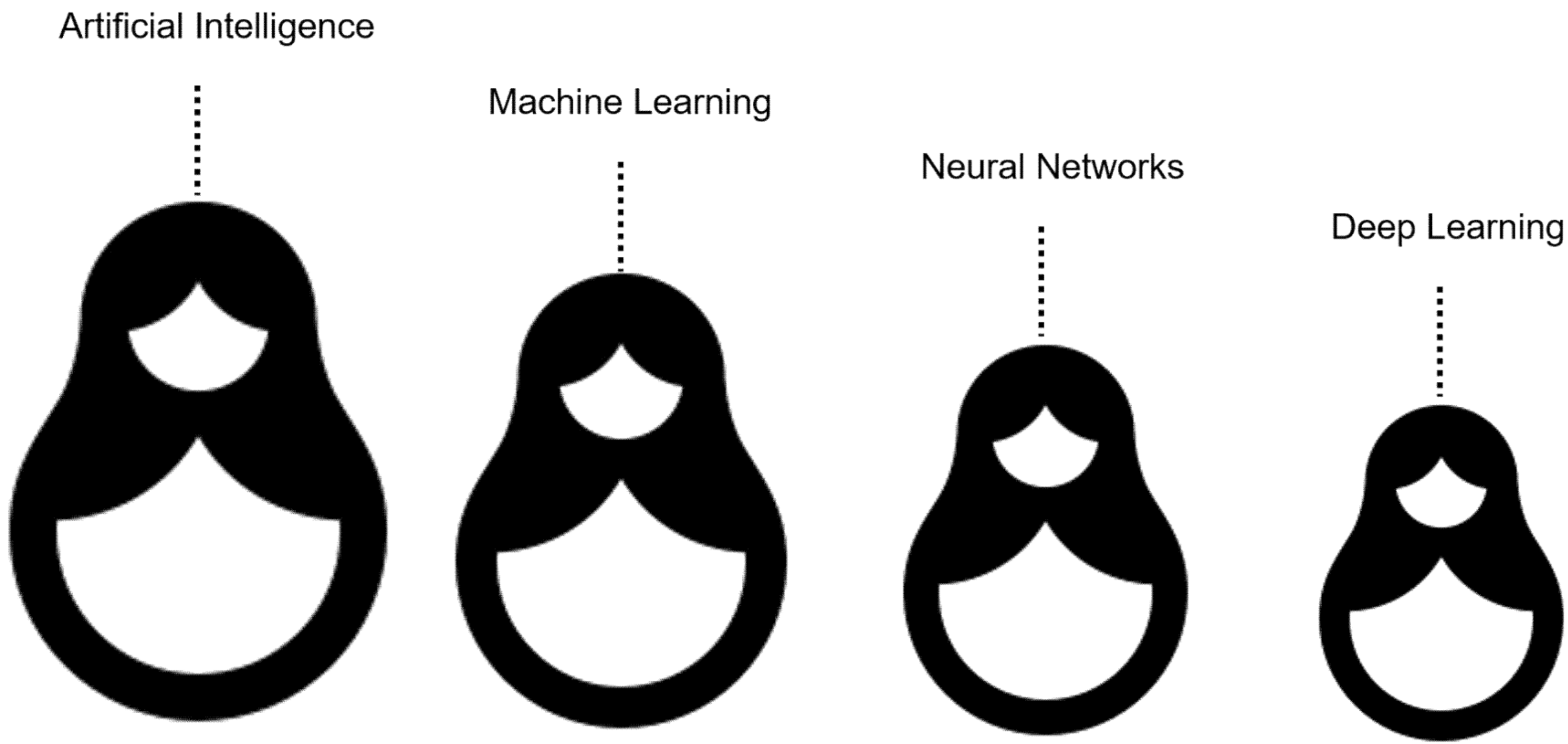

Machine Learning applications: Face Recognition, Computer Vision, Image Classification

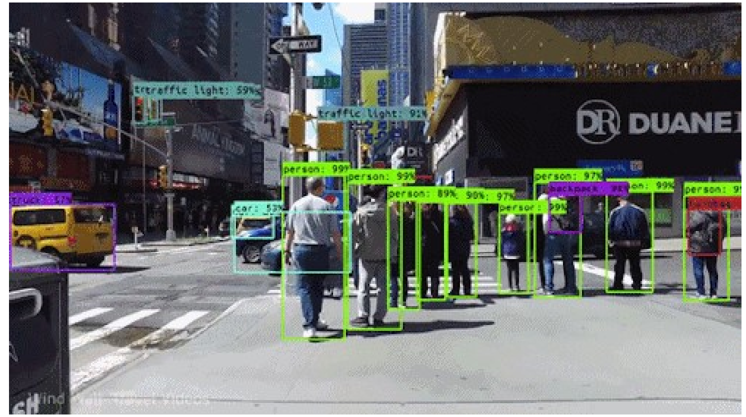

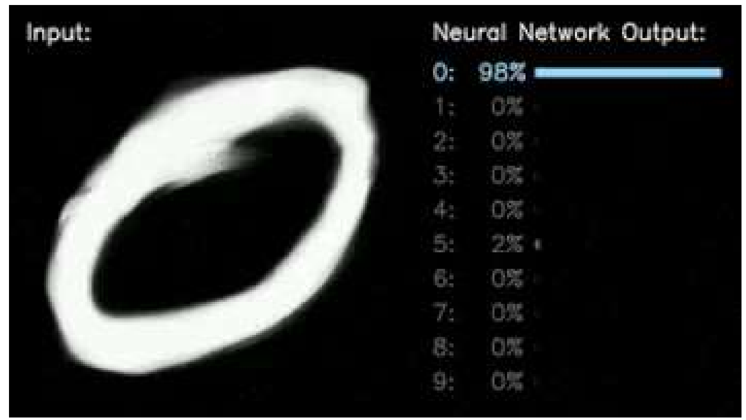

Machine Learning for Pavement Engineering

Università degli Studi di Perugia
Department of Civil and Environmental Engineering

Nicola Baldo
University of Udine

XIX International SIIV Summer School
Perugia 4th - 8th September 2023

Artificial Neural Network: inspired by biological brain

Biological Neural Network Biological Brain

Artificial Neural Network: inspired by biological brain

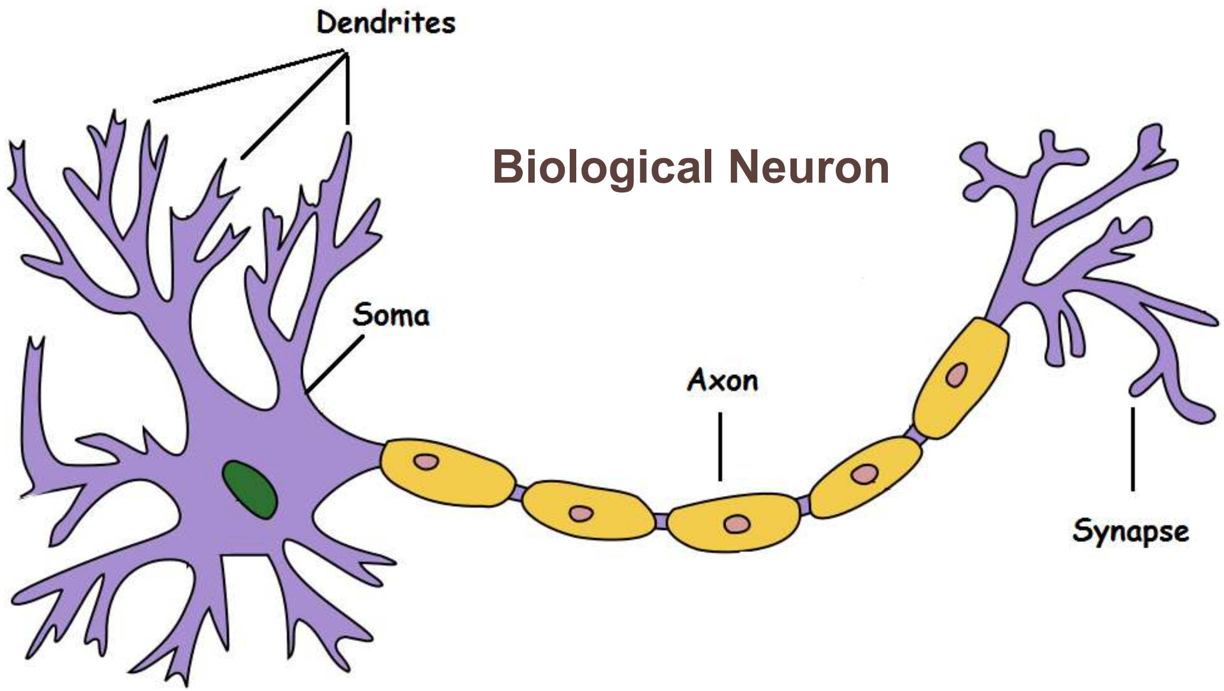

Artificial Neural Network: inspired by biological brain

Feedforward Network

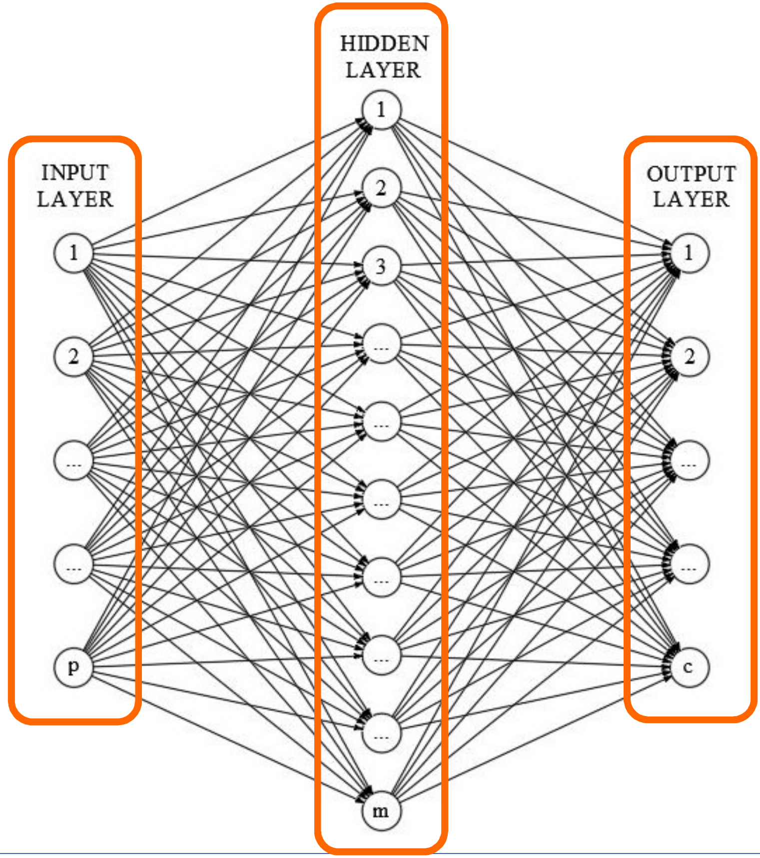

Neurons operate in parallel and are organized into interconnected layers.

Each layer is characterized by a different function and a different number of neurons.

Neurons in the same layer do not communicate with each other.

Feedforward Network

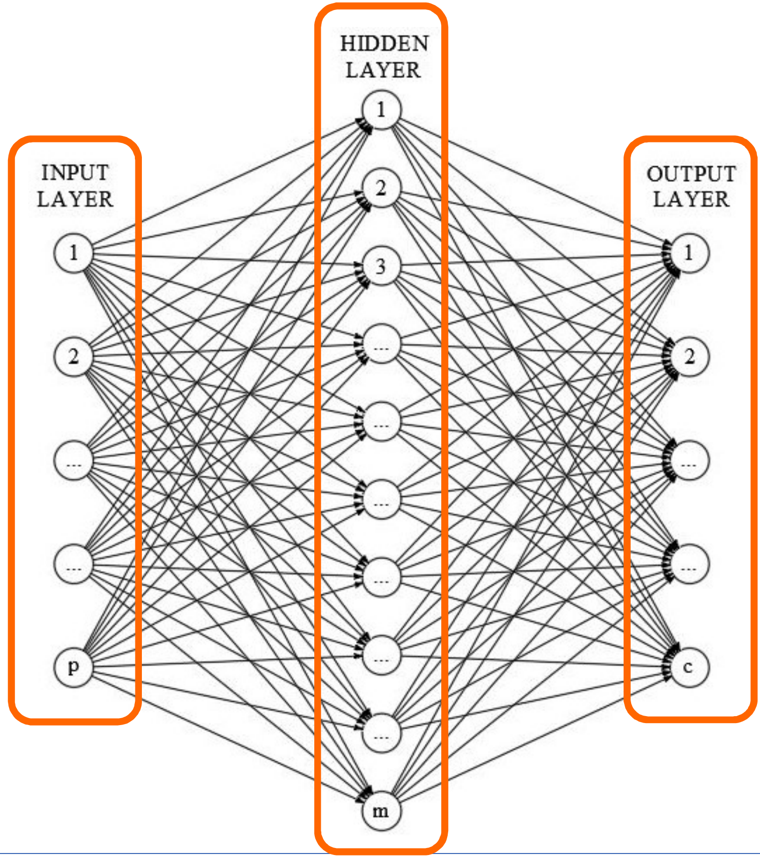

Shallow Neural networks: architecture characterized by only one hidden layer.

Deep learning model: neural network characterized by more than one hidden layers.

Feedforward networks: Information flows only in one direction.

Feedforward Network

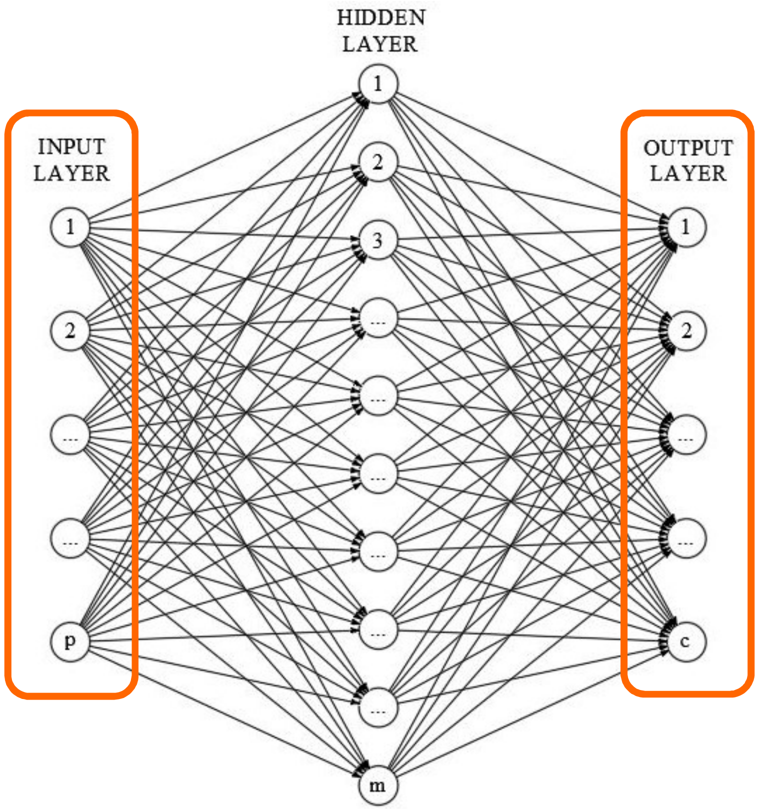

Input layer

$$\bar{\boldsymbol{x}}_{\boldsymbol{i}} = (x_{1i}, x_{2i}, \dots, x_{pi})$$
$$i = 1, \dots, n$$

Output layer

$$\bar{\boldsymbol{y}}_{\boldsymbol{i}} = (y_{1i}, y_{2i}, \dots, y_{ci})$$
$$i = 1, \dots, n$$

Feedforward Network

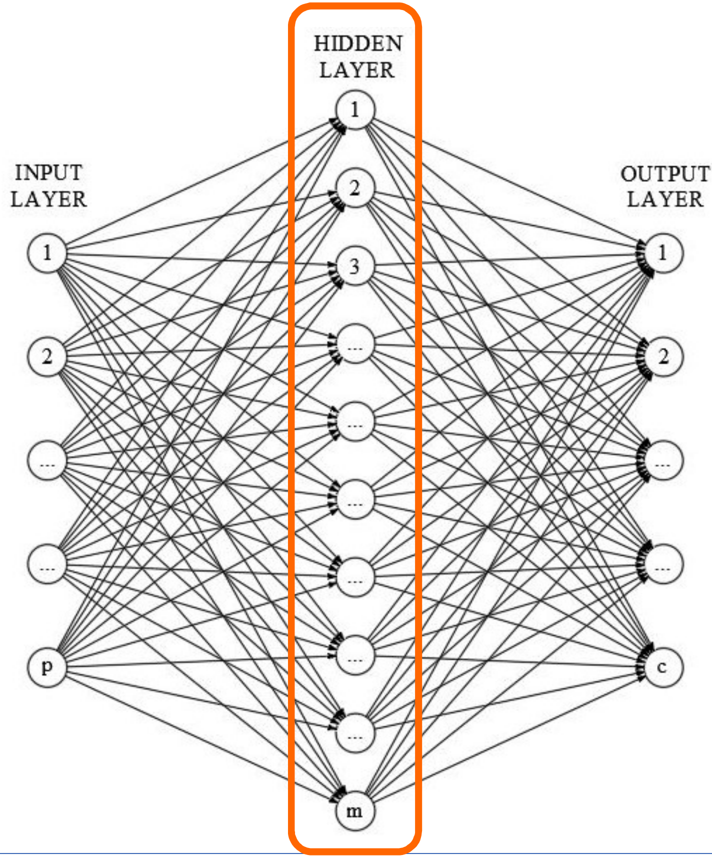

Artificial Neuron: mathematical model by McCulloch and Pitts

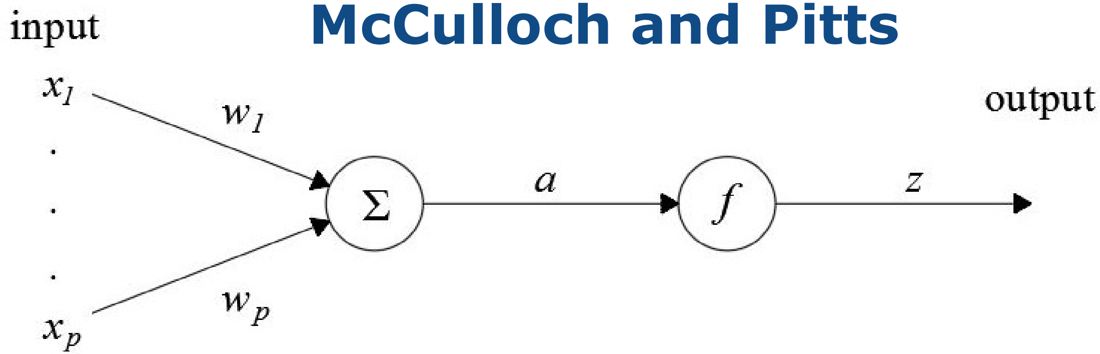

$$a = \sum_{i=0}^{p} w_i x_i$$

$$z = f(a) = f\left(\sum_{i=0}^{p} w_i x_i\right)$$

Biological Neuron

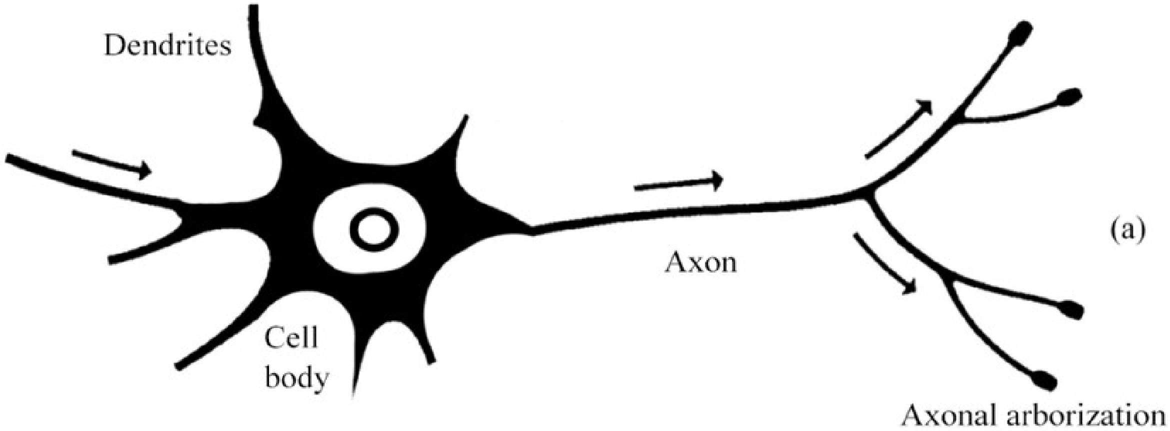

Artificial Neuron: mathematical model by McCulloch and Pitts

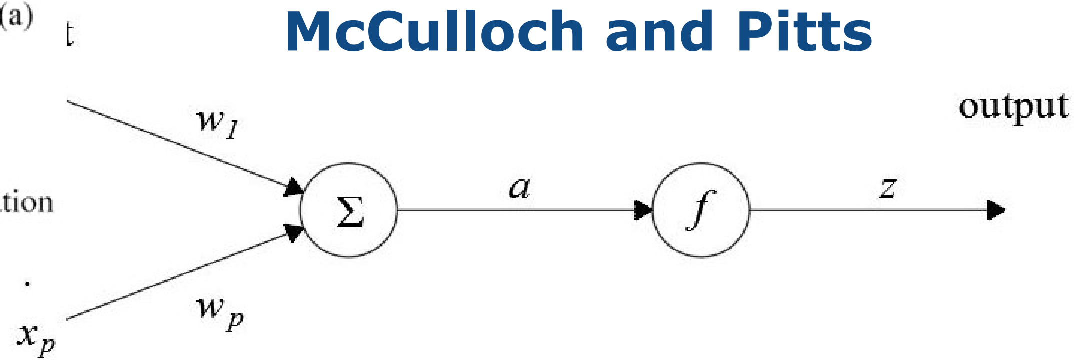

Digital Transition

$$a = \sum_{i=0}^{p} w_i x_i$$

$$z = f(a) = f\left(\sum_{i=0}^{p} w_i x_i\right)$$

Transfer Function

Hyperbolic tangent function

$$f(a) = \frac{e^a - e^{-a}}{e^a + e^{-a}} = \frac{2}{1 + e^{-2a}} - 1$$

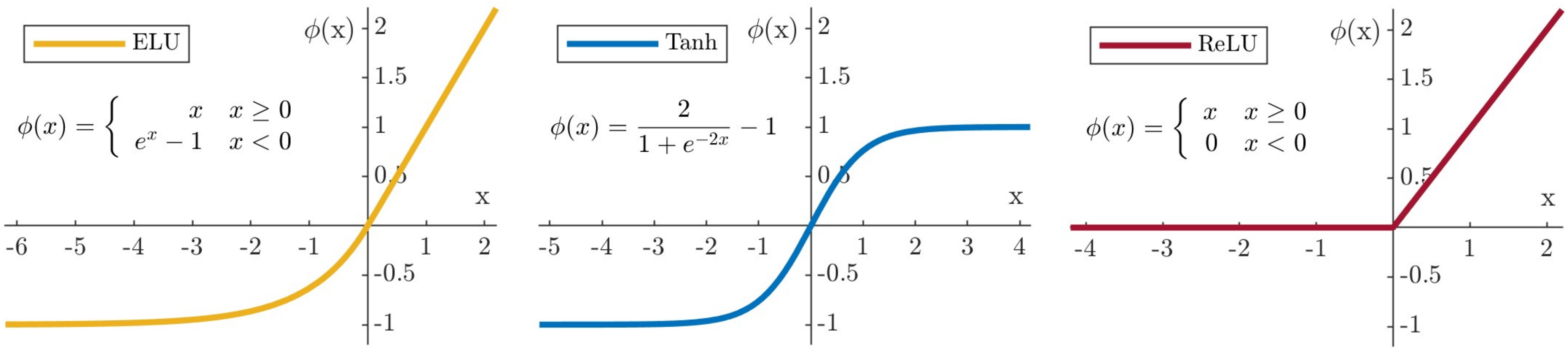

Training procedure

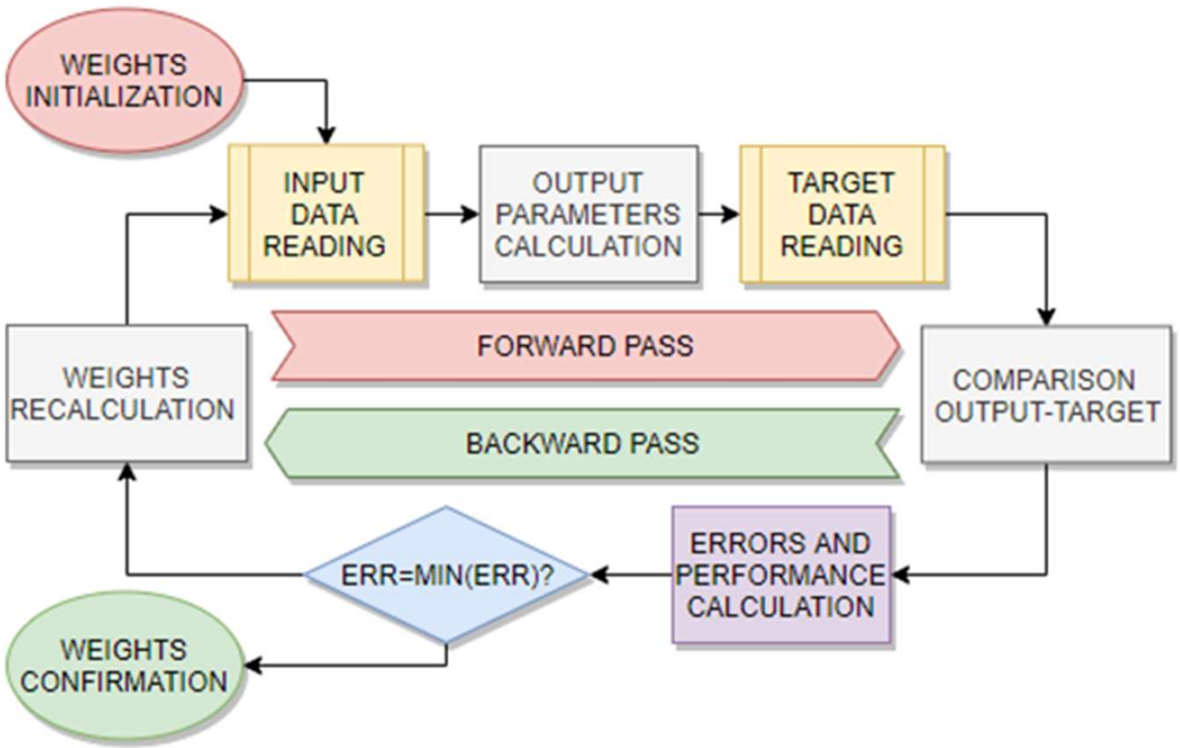

The weights of the connections are defined through a "**training**" process.

In supervised learning, weights are progressively adjusted to minimize the difference between experimental targets and network output, using **backpropagation** algorithms:

- **Gradient Descent**
- **Levenberg–Marquardt**
- **Bayesian Regularization**

Backpropagation Algorithm: Bayesian Regularization

$$\boldsymbol{W}^{e+1} = \boldsymbol{W}^{e} - [\boldsymbol{J}^{T}(\boldsymbol{W}^{e})\boldsymbol{J}(\boldsymbol{W}^{e}) + \boldsymbol{\mu}_{e}\boldsymbol{I}]^{-1}\boldsymbol{J}^{T}(\boldsymbol{W}^{e})\boldsymbol{v}(\boldsymbol{W}^{e})$$

$\boldsymbol{W}$	*Matrix of weights and biases*
$\boldsymbol{e}$	*Generic iteration with* $e \in \{1, \cdots, E\}$
$\boldsymbol{J}$	*Jacobian matrix of training loss function* $F(\cdot)$ *with respect to* $\boldsymbol{W}^{e}$
$\boldsymbol{\mu}$	*Learning step size*
$\boldsymbol{I}$	*Identity matrix*
$\boldsymbol{v}$	*Network errors vector*

$$F(\widehat{\boldsymbol{y}}(\boldsymbol{W}^{e}), \boldsymbol{y}, \boldsymbol{W}^{e}) = \beta \|\widehat{\boldsymbol{y}}(\boldsymbol{W}^{e}) - \boldsymbol{y}\|_2^2 + \alpha \|\boldsymbol{W}^{e}\|_2^2$$

$\boldsymbol{y}$	*Experimental target vector*
$\widehat{\boldsymbol{y}}$	*Predicted output vector*
$\boldsymbol{\alpha}$	*Regularization parameters set according to David MacKay's approach*
$\boldsymbol{\beta}$	

Training process: Underfitting & Overfitting

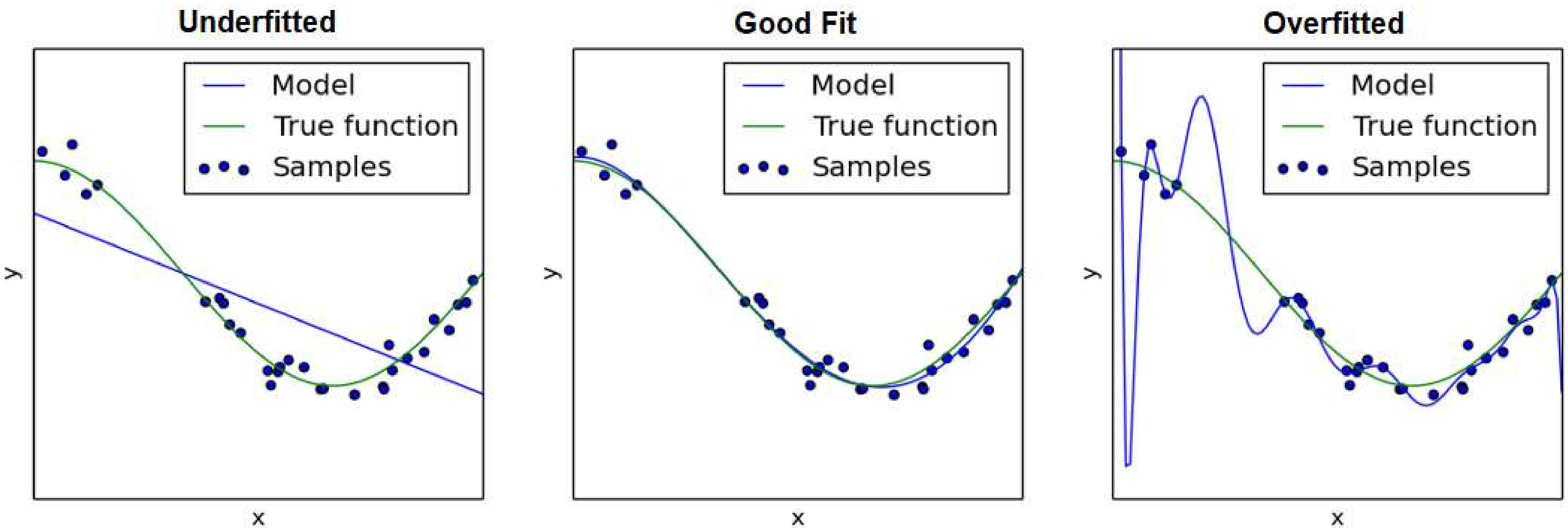

Training process: Data set partition (1/2)

Hold-out Method

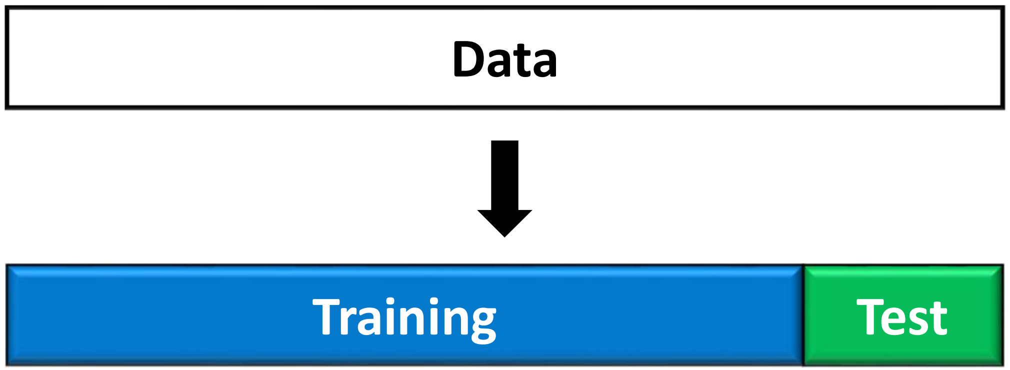

Possibility of running into overfitting phenomenon

With regard to the hold-out method, it is worth pointing out that such a practice has two major drawbacks when the number of observations is small: first, some relevant patterns may be excluded from the training set; second, the training-test splitting makes the model sensitive to the randomness of data in the training set.

Training process: Data set partition (2/2)

Data is here divided into 3 partitions: the first set allows to calculate the loss function; the second one is used to control the model's generalization capabilities during the training process, in order to avoid, possibly, overfitting phenomena. Finally, the third one is used to evaluate the model's predictive capabilities on data it has never seen before.

Early Stopping Procedure

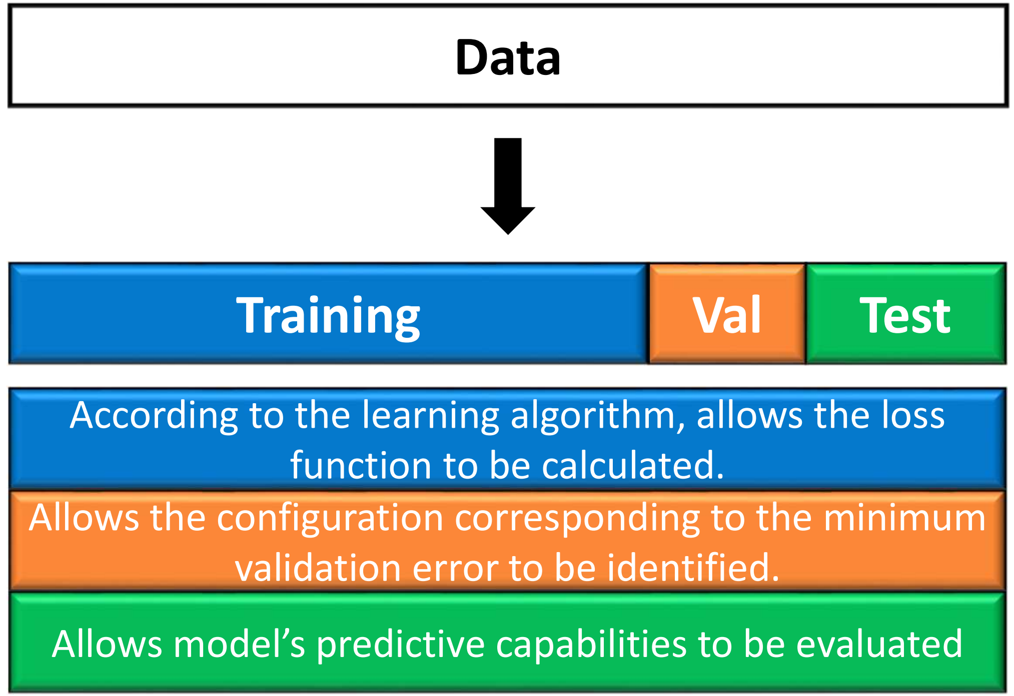

k-fold Cross-Validation

k-fold Cross-Validation is a resampling technique used to elaborate an actual model on a limited data sample. It consists in dividing the data sample in k-partitions. Each sub-sample is used once as validation set and k-1 times as training set. It was decided to give a k-value equal to 5, consistently with the relevant literature.

Randomly Mix Dataset

↓

Split Dataset into k = 5 folds

↓

	Fold 1	Fold 2	Fold 3	Fold 4	Fold 5	
Split 1	Test	Train	Train	Train	Train	Test Score 1
Split 2	Train	Test	Train	Train	Train	Test Score 2
Split 3	Train	Train	Test	Train	Train	Test Score 3
Split 4	Train	Train	Train	Test	Train	Test Score 4
Split 5	Train	Train	Train	Train	Test	Test Score 5

↓

Average the scores obtaining the general performance of the model

ANN Optimization

ANNs models are often based on a network structure set “a priori”.

The search for the optimal network architecture is one of the most difficult tasks in ANN studies and consists of tuning the model settings, called hyperparameters, that yield the best performance score on a validation data-set.

Standard methods are based on random or grid search.

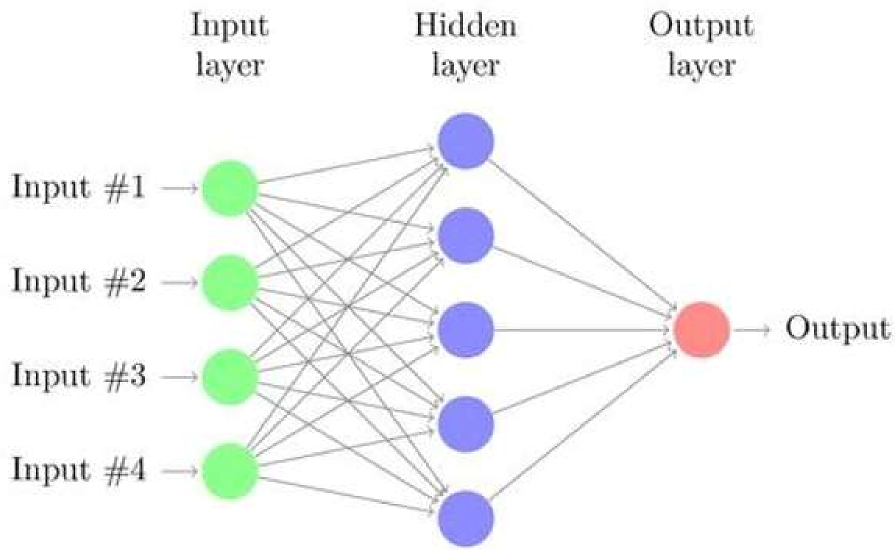

Bayesian Hyperparameters Optimization

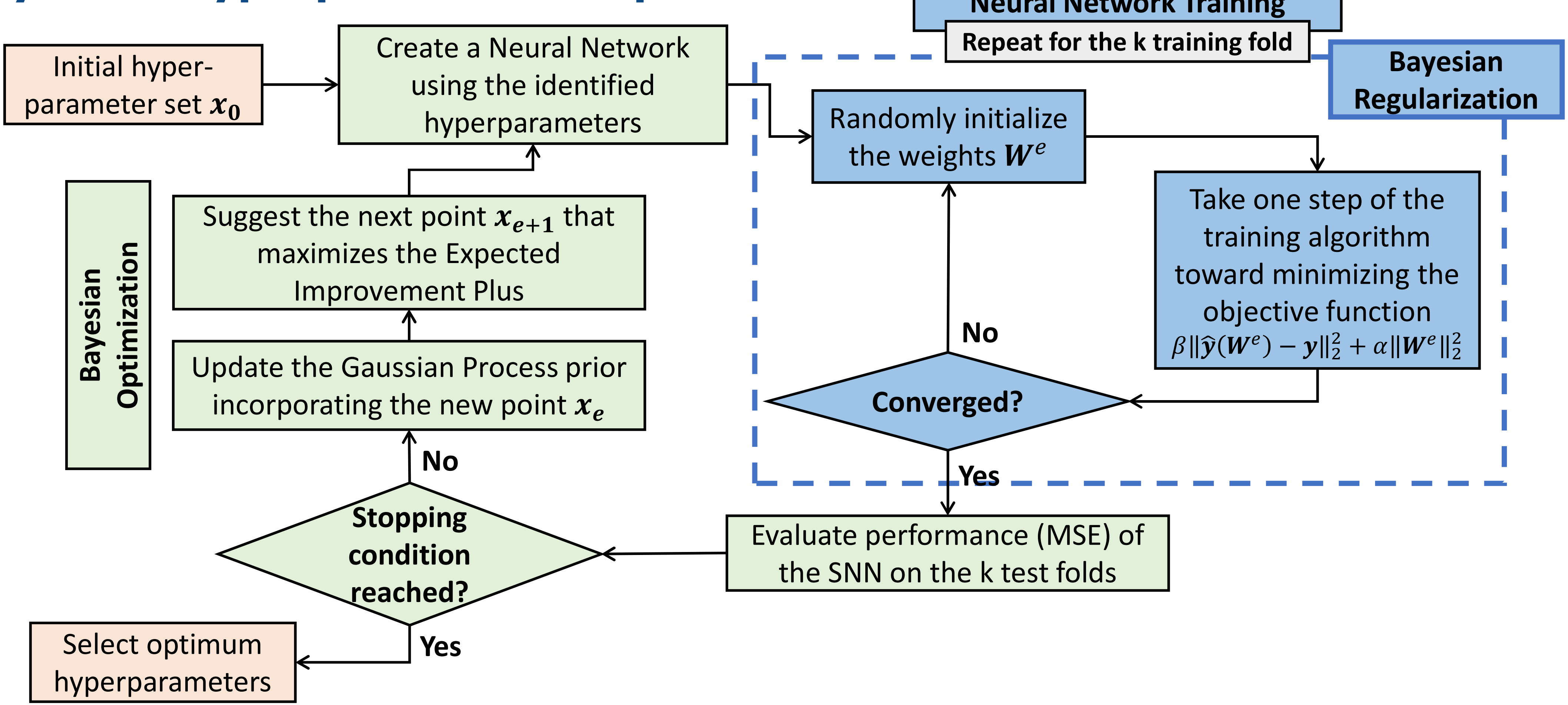

Case study n.1

https://doi.org/10.3311/PPci.19996 | 1
Creative Commons Attribution

Periodica Polytechnica Civil Engineering

Road Pavement Asphalt Concretes for Thin Wearing Layers: A Machine Learning Approach towards Stiffness Modulus and Volumetric Properties Prediction

Nicola Baldo[1*], Matteo Miani[1], Fabio Rondinella[1], Evangelos Manthos[2], Jan Valentin[3]

[1] Polytechnic Department of Engineering and Architecture (DPIA), University of Udine, Via del Cotonificio 114, 33100 Udine, Italy
[2] Department of Civil Engineering, Aristotle University of Thessaloniki, University Campus, 54124 Thessaloniki, Greece
[3] Faculty of Civil Engineering, Czech Technical University, Thákurova 7, 166 29 Prague, Czech Republic
[*] Corresponding author, e-mail: nicola.baldo@uniud.it

Introduction and Scope

- The goal of this study was to implement a data-driven methodology to predict, by means of ANNs, stiffness and volumetric properties of Asphalt Concretes for **VERY THIN** road pavement wearing **LAYERS** (AC-VTL) starting from few compositional variables.

- The experimental data analyzed in this study resulted from investigations carried out at the Highway Engineering Laboratory, Aristotle University of Thessaloniki.

Asphalt Concretes for Very Thin Layers: AC-VTL

- due to its low thickness, requires lesser amount of materials, hence lowers the total cost and **minimizes the quantities of** hard and durable **aggregates** coming **from natural** non-renewable **resources**;
- due to its gap-graded gradation, provides a pavement surface with very good surface characteristics, such as very good macrotexture and (with the use of hard and durable aggregates) very good skid resistance;
- provides a **noise reducing surface** (reduction -3 dB to -4 dB in comparison to conventional dense asphalt concrete surface);
- provides a pavement surface with a certain drainage ability, hence reduction of water spray;
- faster construction can be achieved;
- it can be used as an overlay without milling the underlying layer and not raise the surface level too much;
- up to a certain point it can improve the evenness of the pavement surface, so a levelling course not to be needed;
- in case of maintenance/renewal of the AC-VTL, smaller quantities of materials are wasted or used for recycling;
- no modifications are required by the conventional mixing plants in order to produce AC-VTL.

Materials and Design

AC-VTLs were produced using **diabase aggregates** coming from three different quarries located in Greece.

Property	Value
Los Angeles coefficient (%), EN 1097-2	25
Polished Stone value (%), EN 1097-8	55 to 60
Flakiness index (%), EN 933-3	< 25
Sand Equivalent (%), EN 933-8	> 55
Methylene blue value (mg/g), EN 933-9	< 10 (range of values 6.7 to 8.3)

Materials and Design

Property	Bitumen type	
	50/70	SBS Modified
Penetration (0.1 x mm), EN 1426	64	45
Softening point (°C), EN 1427	45.6	78.8
Elastic recovery (%), EN 13398	–	97.5
Fraas breaking point (°C), EN 12593	– 7.0	– 15.0
After aging		
Retained penetration	–	84
Difference in softening point (°C)	–	– 2.4

Materials and Design

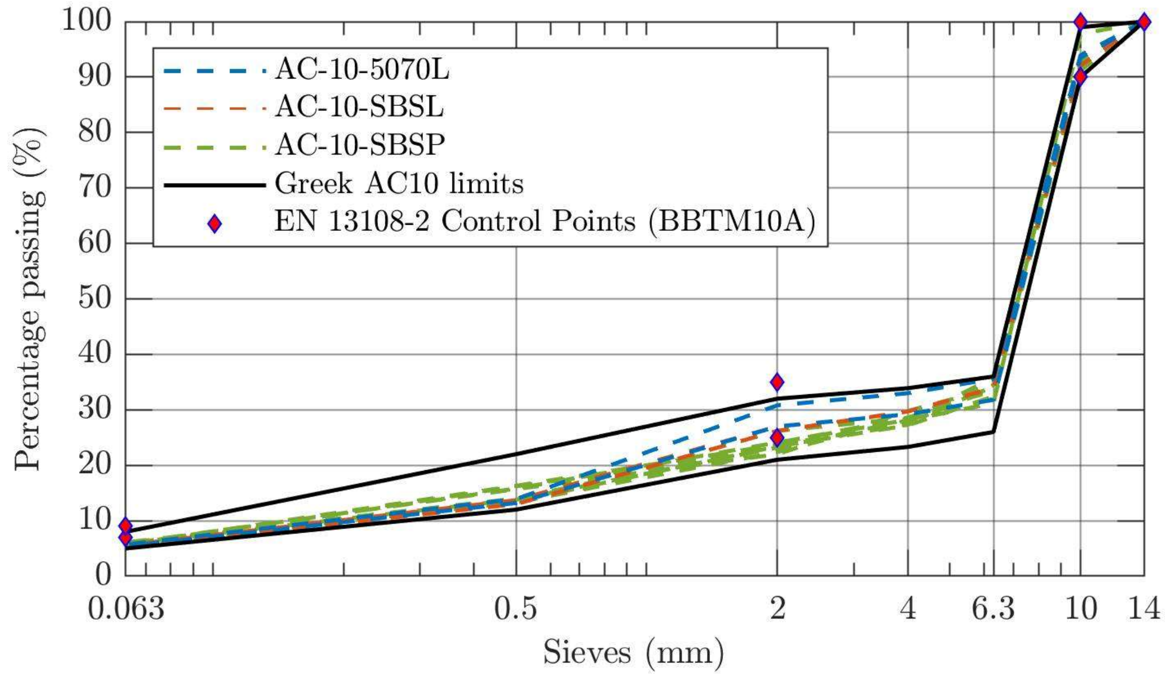

AC-10-5070	30 specimens laboratory-produced using conventional 50/70 bitumen
AC-10-SBSL	30 specimens laboratory-produced using SBS modified bitumen
AC-10-SBSP	32 specimens plant-produced using SBS modified bitumen

Experimental Data AC-10-5070

Cat. Var.	B_C (%)	% 6.3	% 0.063	IT-CY (MPa)	Va (%)	VMA (%)	Cat. Var.	B_C (%)	% 6.3	% 0.063	IT-CY (MPa)	Va (%)	VMA (%)
1	4.12	31.84	5.35	2939	15.7	23.3	1	4.76	35.62	5.71	2750	11.6	20.8
1	4.12	31.84	5.35	2708	15.9	23.5	1	4.76	35.62	5.71	2749	10.7	20.1
1	4.12	31.84	5.35	2944	15.4	23.0	1	5.39	35.62	5.71	2399	9.3	20.1
1	4.76	31.84	5.35	2445	14.2	23.2	1	5.39	35.62	5.71	2355	10.2	20.8
1	4.76	31.84	5.35	2586	14.2	23.1	1	5.39	35.62	5.71	2336	7.1	18.2
1	4.76	31.84	5.35	2441	14.9	23.8	1	6.02	35.62	5.71	1939	7.4	19.7
1	5.39	31.84	5.35	1962	11.1	21.7	1	6.02	35.62	5.71	1964	8.6	20.7
1	5.39	31.84	5.35	1945	11.3	21.8	1	6.02	35.62	5.71	1956	5.5	18.0
1	5.39	31.84	5.35	1921	11.6	22.1	1	5.35	35.62	5.71	2421	9.4	20.0
1	6.02	31.84	5.35	1775	9.3	21.3	1	5.35	35.62	5.71	2354	10.2	20.8
1	6.02	31.84	5.35	1886	9.4	21.4	1	5.35	35.62	5.71	2342	7.2	18.1
1	6.02	31.84	5.35	1965	9.4	21.4	1	6.00	35.62	5.71	1965	7.4	19.7
1	4.12	35.62	5.71	3276	12.7	20.6	1	6.00	35.62	5.71	1957	8.7	20.7
1	4.12	35.62	5.71	3116	17.1	24.5	1	6.00	35.62	5.71	1948	5.5	18.0
1	4.12	35.62	5.71	3227	12.7	20.6							
1	4.76	35.62	5.71	2760	9.6	19.1							

Experimental Data AC-10-SBSL

Cat. Var.	B_C (%)	% 6.3	% 0.063	IT-CY (MPa)	Va (%)	VMA (%)	Cat. Var.	B_C (%)	% 6.3	% 0.063	IT-CY (MPa)	Va (%)	VMA (%)
2	4.41	33.87	5.30	3197	15.6	24.5	2	4.12	31.84	5.60	3356	15.7	23.3
2	4.41	33.87	5.30	3067	17.0	25.8	2	4.12	31.84	5.60	3384	15.3	23.0
2	4.41	33.87	5.30	3278	16.4	25.3	2	4.76	31.84	5.60	3105	14.1	23.1
2	4.79	33.87	5.30	3066	15.6	15.6	2	4.76	31.84	5.60	3085	13.9	23.0
2	4.79	33.87	5.30	3044	16.3	16.3	2	4.76	31.84	5.60	3078	14.2	23.2
2	4.79	33.87	5.30	2931	13.2	13.2	2	5.39	31.84	5.60	2856	11.1	21.7
2	5.11	33.87	5.30	2840	14.4	24.9	2	5.39	31.84	5.60	2854	11.1	21.7
2	5.11	33.87	5.30	2976	13.1	23.8	2	5.39	31.84	5.60	2841	11.2	21.8
2	5.11	33.87	5.30	2873	15.0	25.5	2	6.02	31.84	5.60	2424	8.9	21.1
2	5.48	33.87	5.30	3226	11.9	23.5	2	6.02	31.84	5.60	2451	8.9	21.0
2	5.48	33.87	5.30	2928	13.2	24.6	2	6.02	31.84	5.60	2456	9.4	21.5
2	5.48	33.87	5.30	3093	12.6	24.1	2	6.10	31.84	5.60	2422	7.9	20.4
2	5.86	31.84	5.60	3123	10.9	23.4	2	6.10	31.84	5.60	2438	8.6	21.0
2	5.86	31.84	5.60	3091	10.9	23.5	2	6.10	31.84	5.60	2468	8.6	20.9
2	5.86	31.84	5.60	3358	12.3	24.6							
2	4.12	31.84	5.60	3452	15.6	23.2							

Experimental Data AC-10-SBSP

Cat. Var.	B_C (%)	% 6.3	% 0.063	IT-CY (MPa)	Va (%)	VMA (%)	Cat. Var.	B_C (%)	% 6.3	% 0.063	IT-CY (MPa)	Va (%)	VMA (%)
3	5.58	33.87	5.63	3382	9.5	18.5	3	5.29	35.00	5.58	3332	13.5	22.2
3	5.58	33.87	5.63	3446	9.3	18.3	3	5.29	35.00	5.58	3388	13.3	21.6
3	5.58	33.87	5.63	3260	9.6	18.7	3	5.29	35.00	5.58	3316	13.6	22.4
3	5.58	33.87	5.63	3617	9.1	18.1	3	5.29	35.00	5.58	3786	13.2	22.6
3	5.27	31.17	5.87	3362	14.1	22.5	3	5.42	32.43	5.37	2862	10.6	20.3
3	5.27	31.17	5.87	3458	13.5	22.2	3	5.42	32.43	5.37	2913	10.5	19.5
3	5.27	31.17	5.87	3421	13.9	22.3	3	5.42	32.43	5.37	2809	10.8	19.3
3	5.27	31.17	5.87	3380	13.9	22.7	3	5.42	32.43	5.37	2896	10.7	19.7
3	5.47	32.02	5.77	2810	10.3	19.5	3	5.15	33.92	5.89	3935	15.2	23.9
3	5.47	32.02	5.77	2842	10.0	18.5	3	5.15	33.92	5.89	4145	14.8	23.2
3	5.47	32.02	5.77	2826	10.1	18.6	3	5.15	33.92	5.89	4197	14.3	22.9
3	5.47	32.02	5.77	2827	10.1	18.6	3	5.15	33.92	5.89	4036	15.0	23.5
3	5.74	33.50	6.12	2655	8.2	16.8	3	5.35	35.77	5.24	3309	12.0	20.5
3	5.74	33.50	6.12	3940	7.1	15.9	3	5.35	35.77	5.24	3296	12.1	21.2
3	5.74	33.50	6.12	3612	7.4	16.1	3	5.40	34.53	5.68	2853	11.1	19.9
3	5.74	33.50	6.12	3448	7.6	16.3	3	5.40	34.53	5.68	2865	11.0	19.9

Artificial Neural Network

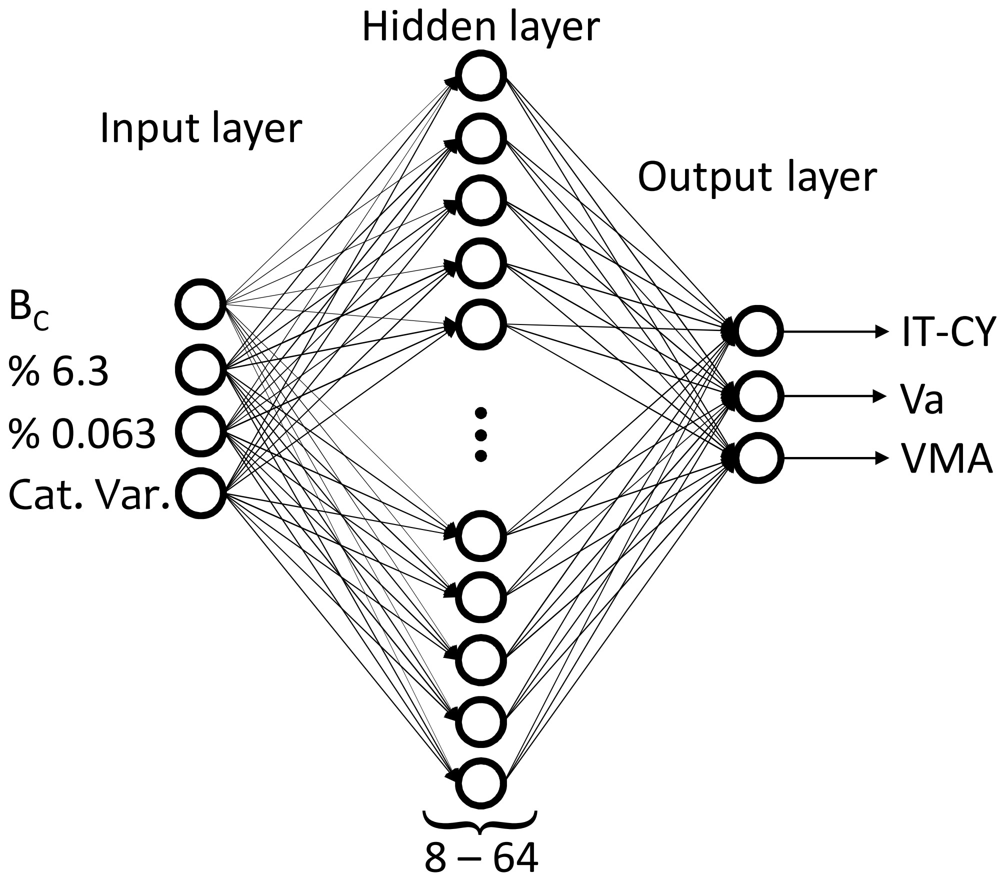

Transfer Function	Equation	Graph
Exponential Linear	$\varphi(x) = \begin{cases} \alpha(e^x - 1) & x \le 0 \\ x & x > 0 \end{cases}$	
Hyperbolic Tangent	$\varphi(x) = \dfrac{e^x - e^{-x}}{e^x + e^{-x}}$	

Input	Description
B_C	Bitumen content (by weight)
% 6.3	% passing at 6.3 mm sieve
% 0.063	% passing at 0.063 mm sieve
Cat. Var.	Categorical variable

Output	Description
IT-CY	Stiffness modulus
Va	Air voids content
VMA	Voids in the mineral aggregate

Hyperparameters Definition

	Hyperparameter	Symbol	Variation Interval
Network Topology	Neurons in the hidden layer	N	$\{8, \cdots, 64\}$
	Transfer Function	act	$\{ELU, Tanh\}$
Learning Algorithm	Learning Rate	μ	$[10^{-4}, 10^{-2}]$
	Increasing factor	μ_{inc}	$[10^{1}, 10^{3}]$
	Decreasing factor	μ_{dec}	$[10^{-3}, 10^{-1}]$
	Maximum Learning Rate	μ_{max}	$[10^{6}, 10^{8}]$
	Learning Algorithm Iterations	E	$\{500, \cdots, 5000\}$

Step-by-step Procedure

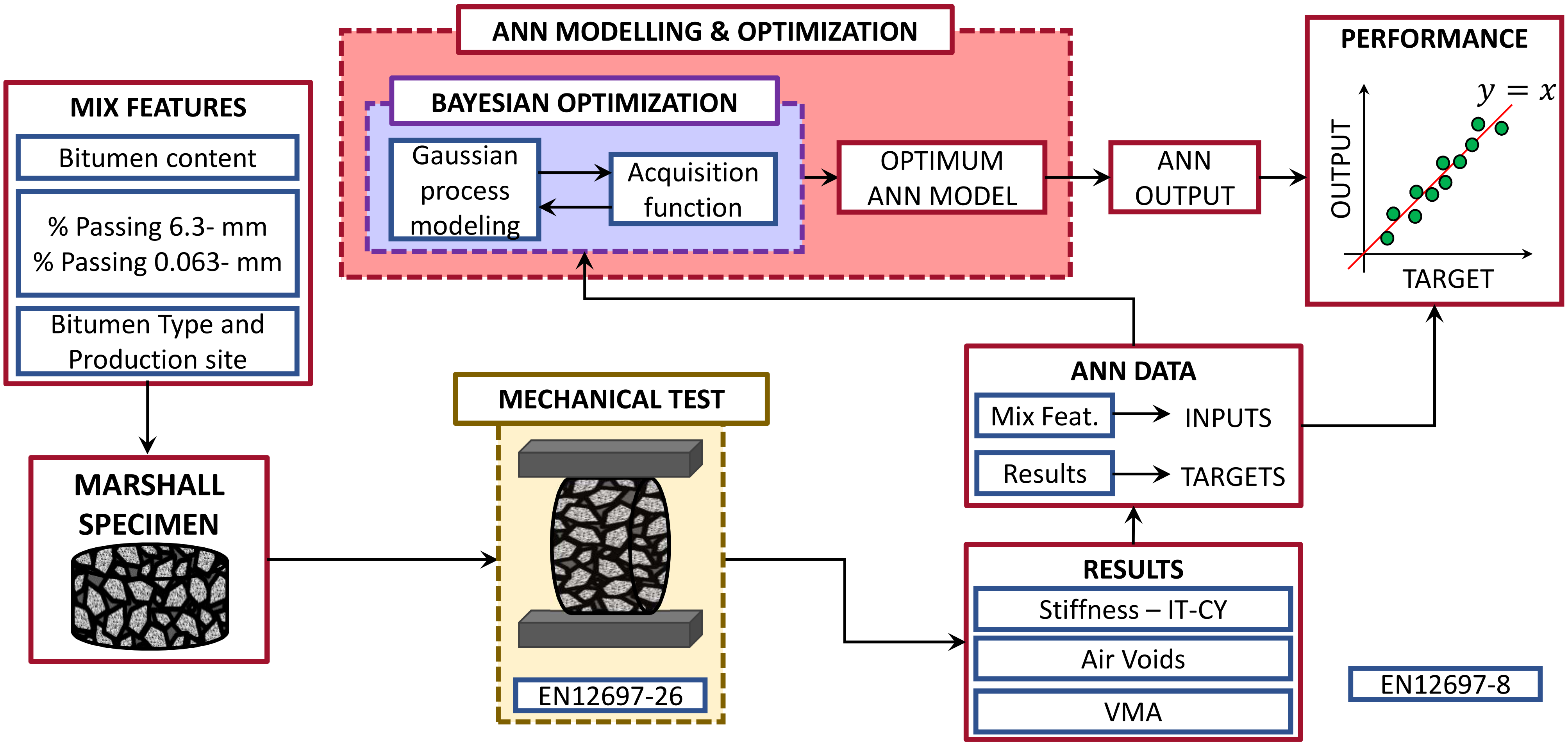

k-fold Cross-Validation

k-fold Cross-Validation is a resampling technique used to elaborate an actual model on a limited data sample. It consists in dividing the data sample in k-partitions. Each sub-sample is used once as validation set and k-1 times as training set. It was decided to give a k-value equal to 8, consistently with the relevant literature. This procedure is iteratively repeated 8 times; finally, the average of the 8 validation scores is given as general performance of the model.

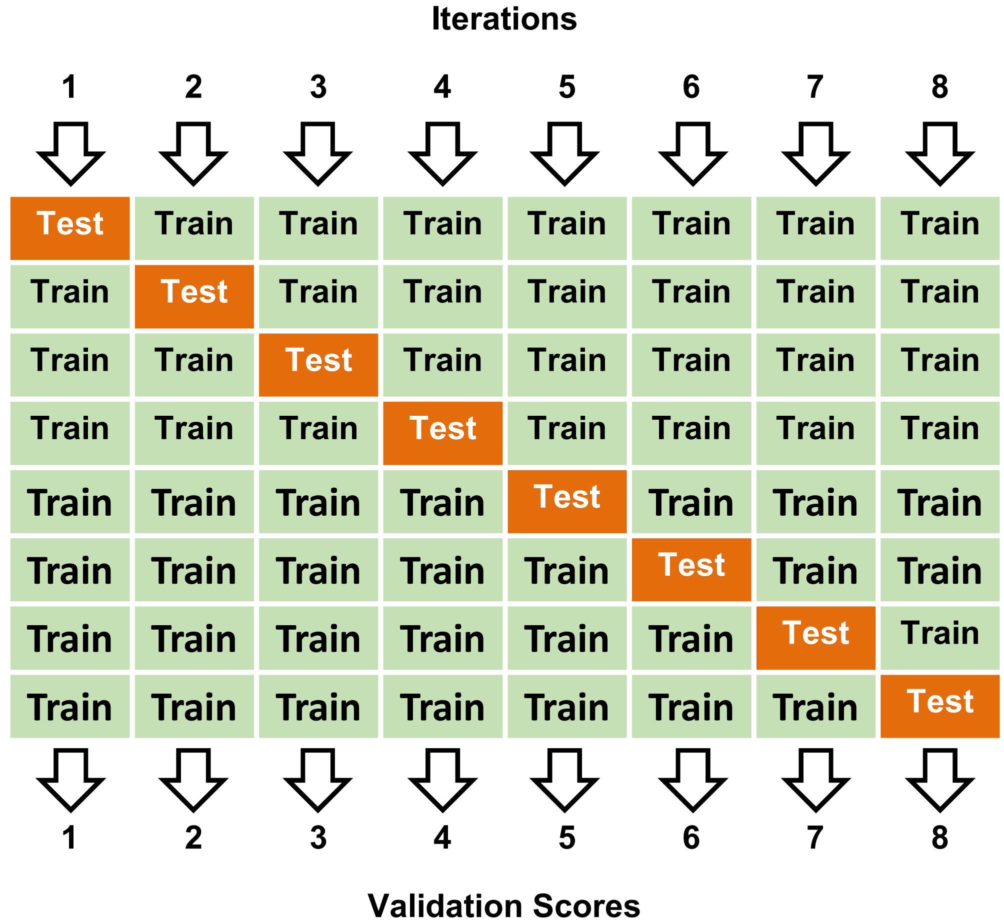

Results and discussion

Feature	Bounded Domain	Selected Value
N	$\{8, \ldots, 64\}$	22
act	$\{Tanh, ELU\}$	$Tanh$
μ	$[10^{-4}, 10^{-2}]$	2.02×10^{-3}
μ_{inc}	$[10^{1}, 10^{3}]$	1.18×10^{2}
μ_{dec}	$[10^{-3}, 10^{-1}]$	1.07×10^{-2}
μ_{max}	$[10^{6}, 10^{8}]$	4.52×10^{7}
E	$\{500, \ldots, 5000\}$	2922

$$F : X_N \times X_{act} \times X_{\mu} \times X_{\mu_{inc}} \times X_{\mu_{dec}} \times X_{\mu_{max}} \times X_E$$

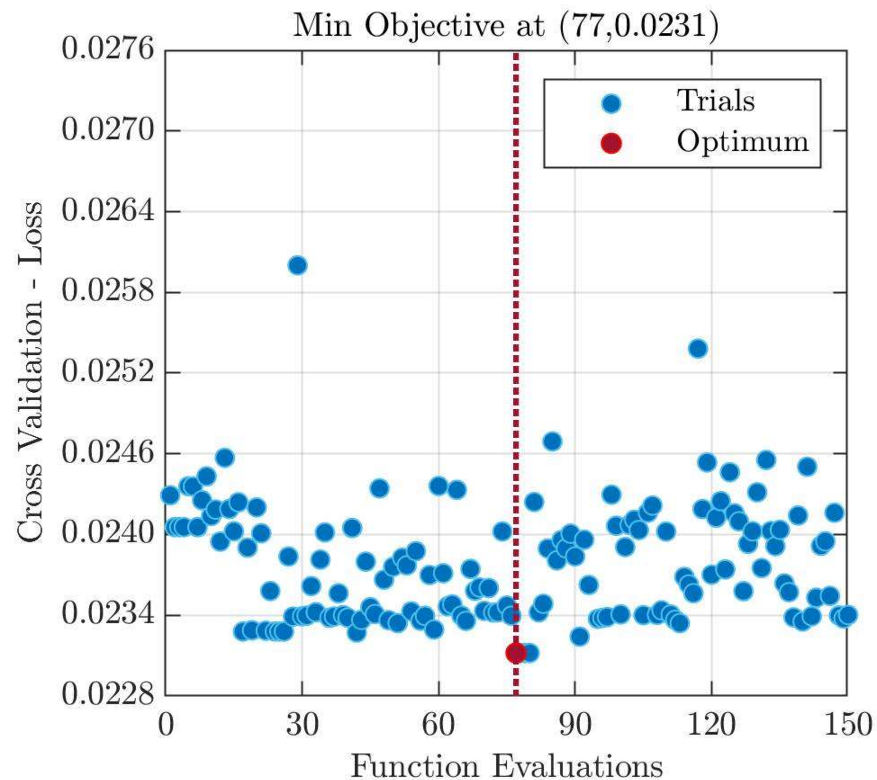

Results and discussion

Fold	Loss (MSE)	R-Pearson coefficient		
		ITSM	Va	VMA
1	0.0172	0.9780	0.9523	0.9374
2	0.0318	0.9654	0.9332	0.9204
3	0.0181	0.9952	0.9413	0.9535
4	0.0273	0.9109	0.9746	0.9630
5	**0.0520**	**0.8698**	**0.8826**	**0.8470**
6	0.0130	0.9856	0.9863	0.9674
7	0.0209	0.9569	0.9470	0.9440
8	**0.0047**	**0.9731**	**0.9975**	**0.9931**
	Average over the 8 test folds			
	0.0231	0.9544	0.9519	0.9407

Results and discussion

Fold	Loss (MSE)	R-Pearson coefficient		
		ITSM	Va	VMA
1	0.0172	0.9780	0.9523	0.9374
2	0.0318	0.9654	0.9332	0.9204
3	0.0181	0.9952	0.9413	0.9535
4	0.0273	0.9109	0.9746	0.9630
5	**0.0520**	**0.8698**	**0.8826**	**0.8470**
8	**0.0047**	**0.9731**	**0.9975**	**0.9931**
6	0.0130	0.9856	0.9863	0.9674
7	0.0209	0.9569	0.9470	0.9440
	Average over the 8 test folds			
	0.0231	0.9544	0.9519	0.9407

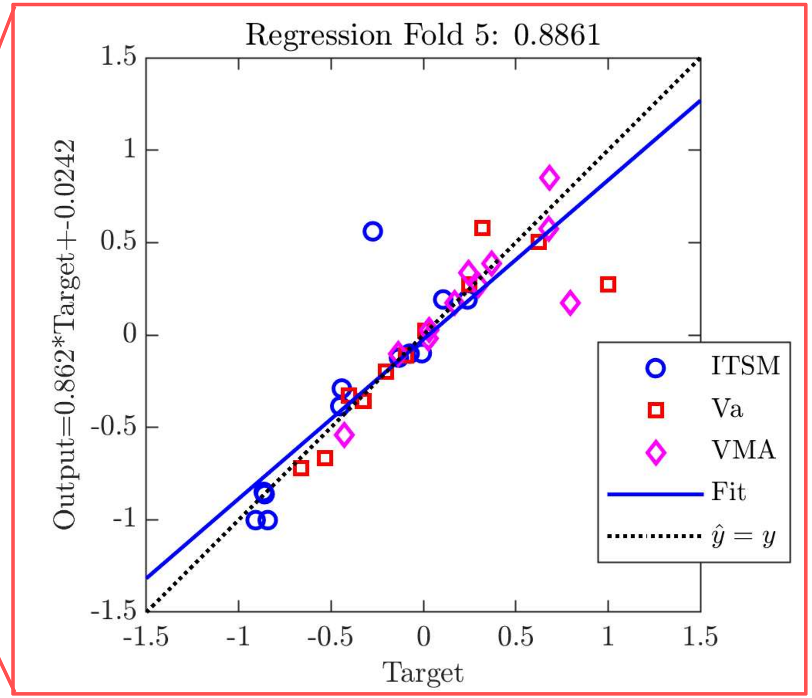

Results and discussion

Fold	Loss (MSE)	R-Pearson coefficient		
		ITSM	Va	VMA
1	0.0172	0.9780	0.9523	0.9374
2	0.0318	0.9654	0.9332	0.9204
3	0.0181	0.9952	0.9413	0.9535
4	0.0273	0.9109	0.9746	0.9630
5	**0.0520**	**0.8698**	**0.8826**	**0.8470**
6	0.0130	0.9856	0.9863	0.9674
7	0.0209	0.9569	0.9470	0.9440
8	**0.0047**	**0.9731**	**0.9975**	**0.9931**
	Average over the 8 test folds			
	0.0231	0.9544	0.9519	0.9407

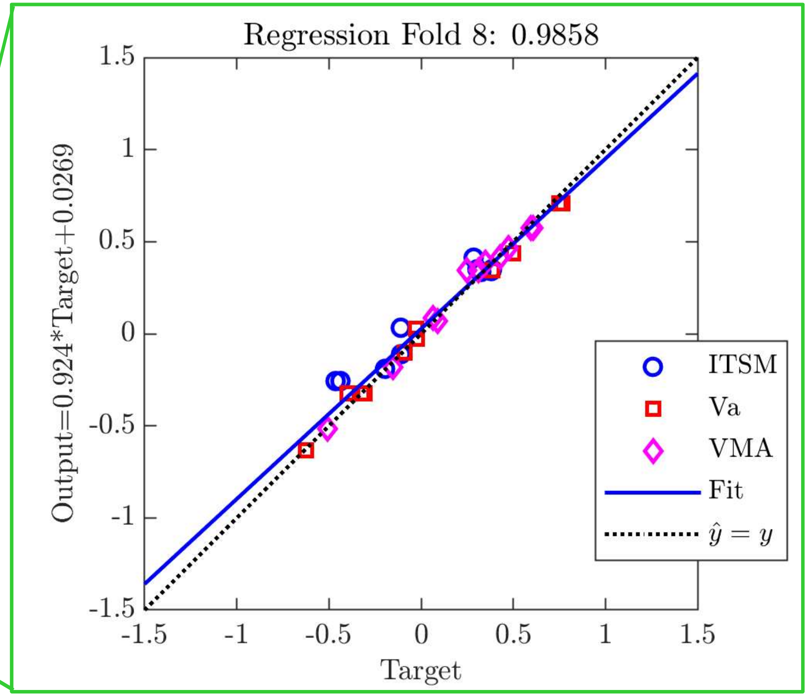

Remarks case study n.1

- It has been feasible to predict simultaneously Stiffness Modulus, Va and VMA, starting from bitumen content, a couple of grading curve data and “the type of mix” categorical variable.
- The best predictions accuracy has been achieved for the Stiffness Modulus.
- The number of artificial neurons in the hidden layer, as well as the hyperparameters values related to the learning algorithm, resulted different with respect to those assumed by default in commercial software or suggested by empirical rules.

Case study n.2

coatings

MDPI

Article

Stiffness Data of High-Modulus Asphalt Concretes for Road Pavements: Predictive Modeling by Machine-Learning

Nicola Baldo [1,*], Matteo Miani [1], Fabio Rondinella [1], Jan Valentin [2], Pavla Vackcová [2] and Evangelos Manthos [3]

[1] Polytechnic Department of Engineering and Architecture (DPIA), University of Udine, Via del Cotonificio 114, 33100 Udine, Italy; matteo.miani@phd.units.it (M.M.); fabio.rondinella@phd.units.it (F.R.)
[2] Faculty of Civil Engineering, Czech Technical University, Thákurova 7, 166 29 Prague, Czech Republic; jan.valentin@fsv.cvut.cz (J.V.); pavla.vackova@fsv.cvut.cz (P.V.)
[3] Department of Civil Engineering, University Campus, Aristotle University of Thessaloniki, 54124 Thessaloniki, Greece; emanthos@civil.auth.gr
* Correspondence: nicola.baldo@uniud.it; Tel.: +39-0432-558-745

Introduction and Scope

- The goal of this study was to predict, by means of ANNs, the stiffness of High-Modulus Asphalt Concretes (HMAC) on the basis of selected input parameters.
- A set of 38 variants of HMAC mixtures was available.
- All mixtures were characterized by a gradation 0–22 mm and had to fulfill requirements set in Czech technical specifications TP 151.
- Hard paving grade 20/30 or PMB 25/55-60 were used.
- Some mix variants contained between 10% and 30% RAP.

Experimental data set
(VMT stands for Vysokým Modulem Tuhosti, i.e., HMAC in Czech)

Mix	Bitumen Type	ID	Bulk Density	Max Bulk Density	Binder Content	Voids Content	Maximum Strength	Marshall Stability	Marshall Flow	IT-CY 15 °C
			(g/cm^3)	(g/cm^3)	(%)	(%)	kN	kN	(0.1 mm)	(MPa)
VMT 22 with 30% RA (Froněk-A)	20/30	M1	2.455 2.429 2.456	2.640	4.9 4.9 4.9	7.0 8.0 7.0	20.6 22.4 21.6	20.0 22.7 23.1	33 35 28	16,062 14,283 16,078
VMT 22 with 30% RA (Froněk-B)	20/30	M1	2.459 2.453 2.456	2.647	4.6 4.6 4.6	7.1 7.3 7.2	20.7 19.6 21.0	20.9 20.5 21.4	51 41 43	14,867 15,616 14,350
VMT 22 with 30% RA (Froněk-C)	20/30	M1	2.473 2.475 2.485	2.663	4.3 4.3 4.3	7.2 7.0 6.7	22.8 24.7 24.1	22.4 25.9 24.6	22 24 27	15,974 15,535 15,452
VMT 22 with 20% RA (Froněk-1)	20/30	M2	2.467 2.463 2.461	2.676	4.3 4.3 4.3	7.8 8.0 8.0	20.1 19.0 20.2	20.5 19.8 21.0	58 42 30	12,049 14,419 13,003
VMT 22 with 20% RA (Froněk-2)	20/30	M2	2.486 2.462 2.480	2.682	4.6 4.6 4.6	7.3 8.2 7.5	20.7 18.9 19.6	21.7 20.0 19.8	59 42 47	13,792 11,559 12,452
VMT 22 with 20% RA (Froněk-4)	20/30	M2	2.460 2.460 2.443	2.678	4.9 4.9 4.9	8.1 8.1 8.8	23.5 24.3 23.9	23.5 23.9 24.6	53 45 30	14,441 15,113 16,558
VMT 22 with 20% RA (Froněk-6)	20/30	M2	2.422 2.411 2.422	2.667	5.2 5.2 5.2	9.2 9.6 9.2	18.6 19.1 22.3	21.8 22.2 25.4	35 27 34	13,116 11,548 12,370

Experimental data set

(VMT stands for Vysokým Modulem Tuhosti, i.e., HMAC in Czech)

Mix	Bitumen Type	ID	Bulk Density (g/cm³)	Max Bulk Density (g/cm³)	Binder Content (%)	Voids Content (%)	Maximum Strength kN	Marshall Stability kN	Marshall Flow (0.1 mm)	IT-CY 15 °C (MPa)
VMT 22 with 30% RA var. 5.1	50/70	M3	2.547 2.554 2.538	2.617	5.1 5.1 5.1	2.7 2.4 3.0	17.1 17.2 19.6	19.7 20.0 21.9	71 55 45	13,171 11,659 13,242
VMT 22 with 30% RA. var. 4.8	50/70	M3	2.538 2.535 2.539	2.607	4.8 4.8 4.8	2.6 2.8 2.6	17.4 14.8 22.7	19.9 16.9 25.5	58 47 61	12,739 13,287 13,217
VMT 22 with 30% RA (Froněk)	50/70	M3	2.549 2.539 2.548	2.602	4.8 4.8 4.8	2.0 2.4 2.1	17.4 15.3 16.8	20.2 17.9 19.0	53 63 66	13,025 14,267 13,325
VMT 22 with 30% RA (Froněk)	50/70	M3	2.553 2.548 2.548	2.626	4.6 4.6 4.6	2.8 3.0 3.0	20.6 18.6 20.2	20.7 21.0 23.4	51 54 50	15,871 15,666 16,707
VMT 22 with 20% RA (Froněk-3)	50/70	M4	2.473 2.495 2.477	2.639	4.8 4.8 4.8	6.3 5.4 6.1	18.1 20.2 21.5	19.0 21.6 22.3	34 34 46	12,729 12,282 14,101
VMT 22 with 20% RA (PKB-A)	50/70	M4	2.397 2.421 2.412	2.496	4.4 4.4 4.4	4.0 3.0 3.4	14.2 13.4 12.2	13.6 13.4 12.4	48 50 51	8666 9064 8135
VMT 22 with 10% RA (PKB-101)	50/70	M5	2.358 2.351 2.355	2.559	4.6 4.6 4.6	7.9 8.1 8.0	12.1 15.3 12.8	11.4 14.1 14.5	35 37 34	8950 9339 9311
VMT 22 with 10% RA (PKB-102)	50/70	M5	2.341 2.343 2.323	2.559	4.5 4.5 4.5	8.5 8.4 9.2	17.1 17.1 15.1	16.2 16.1 14.2	90 80 96	9203 9142 9361

Stiffness prediction based on Marshall test results

Marshall test
(EN 12697-34)
Empirical

Stiffness Modulus test
(EN 12697-26)
Performance based

The Procedure

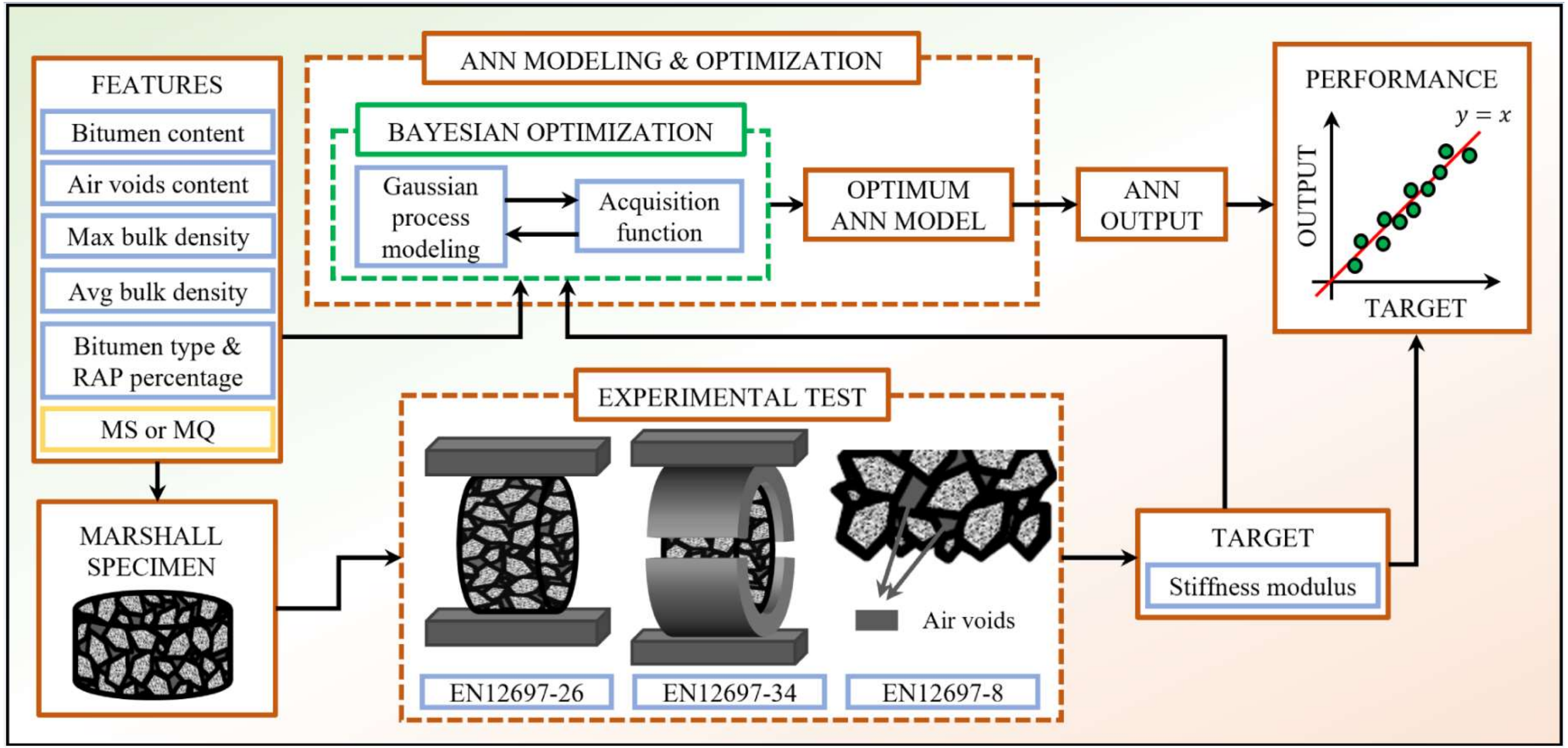

Hidden Neuron

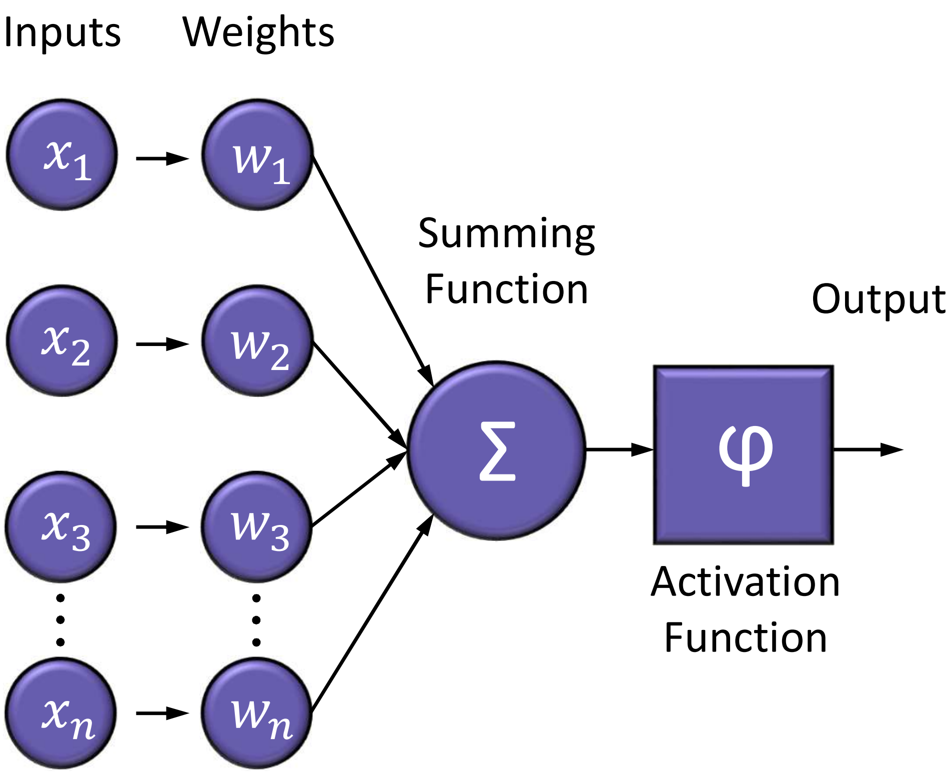

Activation Function	Equation	Graph
Rectified Linear	$\varphi(x) = \begin{cases} 0 & x \leq 0 \\ x & x > 0 \end{cases}$	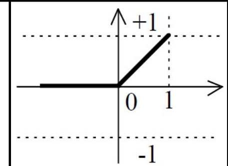
Hyperbolic Tangent	$\varphi(x) = \dfrac{e^x - e^{-x}}{e^x + e^{-x}}$	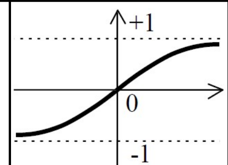
Logistic Sigmoid	$\varphi(x) = \dfrac{1}{1 + e^{-x}}$	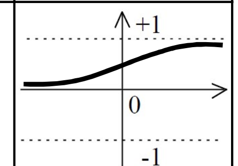

The k-fold Cross Validation

A set of n observations is randomly split into five non-overlapping groups. Each of these fifths acts as a validation set (shown in beige), and the remainder as a training set (shown in blue). The test error is estimated by averaging the five resulting MSE estimates.

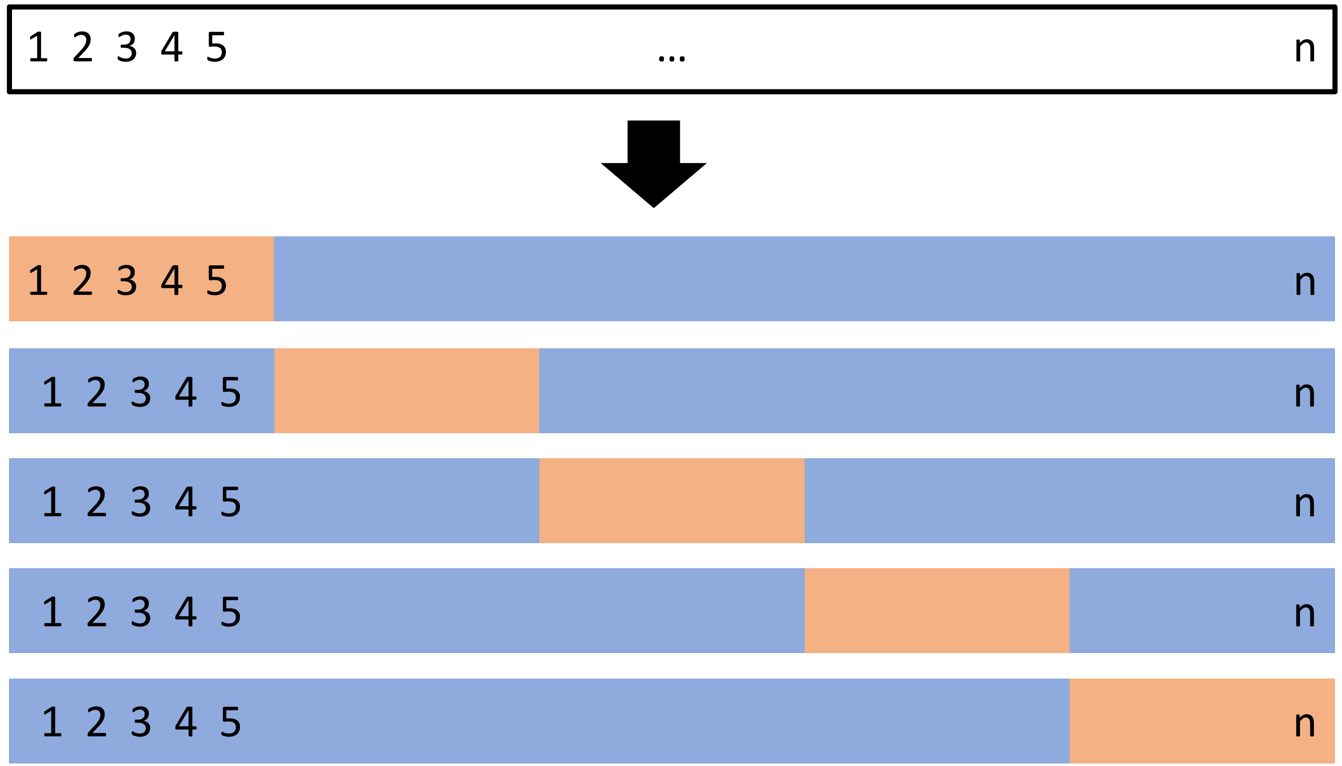

Results

In general, the addition of the empirical mechanical parameters among the predictors of the stiffness modulus improved the prediction accuracy compared to the use of mixes' composition parameters alone, as shown by the model evaluation functions: in particular, the values of the R^2_{adj} parameter, a modified version of R^2 which assesses the effect of adding predictors to a model, increase with the use of MS or MQ, showing that the new independent term improves the model more than would be expected by chance, but the percentage gain in model accuracy is really paltry. In fact, although the percentage variation in MAE between MIX_{SNN} and MS_{SNN} is +23.4%, in terms of R^2_{adj} the gain is only +0.29% and therefore such that it may not justify the use of additional data, such as any results of the Marshall test.

ID	Features	N	ϕ	$f(\cdot)$	MAE	RMSE	R^2	R^2_{adj}
MIX_{SNN}	5	6	TanH	12.093	209.12	293.56	0.9909	0.9894
MS_{SNN}	6	6	TanH	11.856	160.17	241.54	0.9938	0.9923
MQ_{SNN}	6	8	LogS	12.373	174.91	272.61	0.9922	0.9902

Results

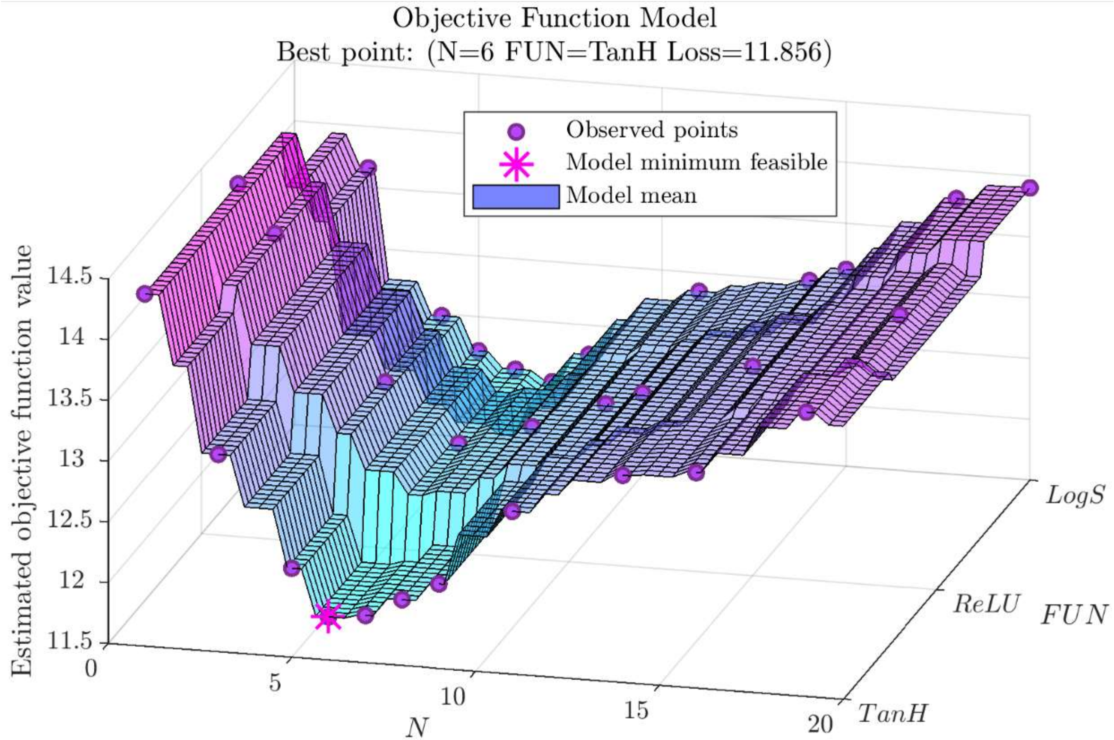

Objective Function Model
Best point: (N=6 FUN=TanH Loss=11.856)
Observed points
Model minimum feasible
Model mean
Estimated objective function value
14.5
14
13.5
13
12.5
12
11.5
0
5
10
15
20
N
LogS
ReLU
TanH
FUN

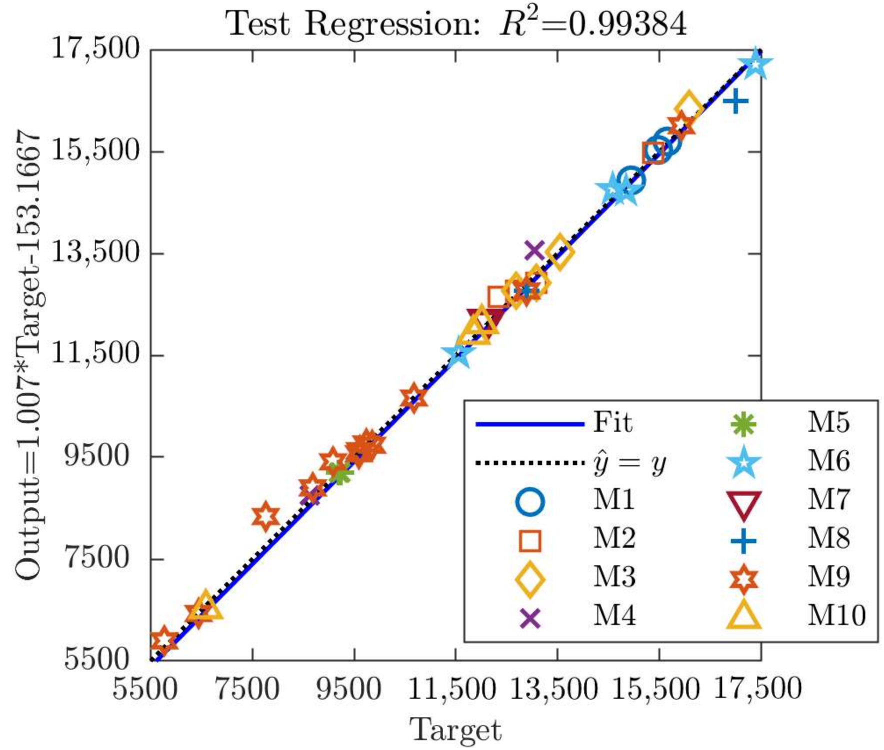

Test Regression: R^2=0.99384
Output=1.007*Target-153.1667
Target
17,500
15,500
13,500
11,500
9500
7500
5500
Fit
$\hat{y} = y$
M1
M2
M3
M4
M5
M6
M7
M8
M9
M10

Remarks case study n.2

- It has been feasible to fit experimental data of asphalt concretes partially made with RAP.

- The inclusion in the input data of Marshall Stability or Quotient values, allows to improve the prediction accuracy of the Stiffness Modulus.

- For each of the neural models analyzed, the Bayesian optimization procedure has identified a different combination of hidden neurons and transfer functions.

Case study n.3

6th World Multidisciplinary Civil Engineering · Architecture · Urban Planning Symposium

WMCAUS 2021

30 August-3 September, 2021 - Prague (Czech Republic)

www.wmcaus.org

Performance Prediction of Fine-Grained Asphalt Concretes with Different Quarry Fillers by Machine Learning Approaches

Authors: Nicola BALDO, Matteo MIANI, Fabio RONDINELLA, Pavla VACKOVÁ, Jan VALENTIN
Address: Udine, Italy & Prague, Czech Republic

Introduction and scope

- The main goal was the **prediction of the stiffness** of asphalt concretes, prepared with different quarry fillers used as alternatives for traditional limestone filler, by Machine Learning approaches which consider the chemical properties of the selected fillers and the quarry aggregate types as input variables.

- The case study involved several fillers and stone aggregates that were used to produce Marshall specimens of a specific fine-grained asphalt concretes designed originally for the assessment of filler suitability in terms of adhesion phenomenon.

Materials – Aggregates

Aggregates from the **three quarries** were chosen for adhesion evaluation both because of their availability **in the Czech Republic** and regular use for HMA production, and also because of their surface properties and petrographic composition of the parent rock. This selection includes aggregates exhibiting diverse adhesion to bituminous binders.

Brant

The aggregate from the Brant quarry contains **granite porphyry** as the key mineral. Despite its porous surface due to weathering, it is also **hydrophilic** and therefore susceptible to stripping.

Chlum

The aggregate from the Chlum quarry can be classified as acid leachate (**phonolite**). Feldspars cannot be detected macroscopically, biotite may be present in small amounts. Aggregates produced from this rock are generally classified as **hydrophilic**, exhibiting poor bitumen aggregate adhesion; Suitable adhesion promoters are usually required in the mix design or, if possible, this aggregate is avoided.

Zbečno

The host rock in Zbečno quarry is igneous. From a petrographic point of view, it is a **spilite** which contains plagioclase strips (andesine) and isometric grains of pyroxenes. Secondary veins with quartz, calcite, chlorite or pumpellyite are abundant. Some spilites contain up to 3 mm of feldspar growth. Zbečno aggregate usually exhibits good bitumen-aggregate adhesion.

Materials – Bitumen

Soft paving grade bitumen 160/220 with a penetration of 187 dmm and a softening point of 38 °C was used in this study. The use of this type of binder is required by the test protocol given in EN 1744-4, Annex A.

Materials – Filler

As alternative fillers used to replace the traditional limestone filler, several variants of quarry dust or **backhouse fillers from asphalt mix production** representing different quarries or in two cases asphalt mixing plants were chosen. Quarry dust (QD) came from the quarries of Plešovice, Litice, Chrtníky, and Chornice. The backhouse filler (BF) was collected from the Brant (Fronˇek) and Kladno (PKB) asphalt plants.

Materials - XRF spectrometry

X-ray fluorescence (XRF) spectrometry was used to determine percentages of most important oxides in filler samples with focus mainly on SiO_2 and CaO. It is established that if the sample contains more than 65% of SiO_2, the rock is of acidic origin and usually hydrophilic. On the other hand, presence of CaO indicates that the material is hydrophobic.

Most important oxides in filler samples determined through XRF spectrometry.

Compound	BF Brant m/m%	BF PKB m/m%	QD Plešovice m/m%	QD Litice m/m%	CaCO3 (reference) m/m%	QD Chrtníky m/m%	QD Chornice m/m%
SiO2	57.35	53.98	70.27	36.35	2.86	34.40	60.97
Al2O3	21.35	18.98	13.88	16.93	5.09	18.39	20.57
Fe2O3	9.14	8.40	3.86	10.34	0.55	16.10	3.65
CaO	1.28	6.91	1.55	22.34	65.40	12.92	4.35
MgO	3.65	3.95	0.74	9.42	24.55	15.01	2.39

Materials – Asphalt Concretes

The asphalt concrete variants (21) had the same material composition and mix design: filler content was fixed at 10% by mass of the mix, the grading curve is roughly the same, the bitumen is about 6% by mass of the mix.

Six Marshall test specimens have been compacted at 140°C by 2x25 blows (used for water resistance evaluation), six Marshall test specimens compacted at 140°C by 2x50 blows (used for Marshall test, ITS and stiffness determination) and about 1 kg was used for determining maximum density according to EN 12697-5. The six test specimens with lower compaction energy were later used for the water susceptibility test according to EN 12697-12. The conditioning according to EN 1744-4, annex A shall be in water bath at 40±1°C for 48h.

Strength, durability and stiffness

Quarry	Asphalt Mixture	Marshall Stability [kN]	S_{MA}	Marshall Stiffness [kN/mm]	MT_{ratio}	Stiffness @ 15°C [MPa]	ITS [MPa]	ITSR
Brant	Reference ($CaCO_3$)	9.9 10.1	-1.7 %	3.88 3.56	0.08	3 808	1.35 1.22	91 %
	BF PKB	7.8 5.9	24.0 %	4.16 2.31	0.44	3 193	1.16 1.05	91 %
	BF Brant	9.5 7.6	19.7 %	4.44 2.86	0.36	4 284	1.12 1.04	93 %
	QD Plešovice	9.4 9.5	-0.7 %	4.62 4.19	0.09	4 571	1.47 1.15	78 %
	QD Chrtníky	9.1 6.3	30.8 %	4.79 2.55	0.47	4 503	1.00 0.73	73 %
	QD Litice	8.7 8.2	5.8 %	4.00 4.09	-0.02	3 242	1.18 0.94	80 %
	QD Chornice	14.9 10.3	30.9 %	5.73 3.21	0.44	5 255	1.53 1.00	65 %

Strength, durability and stiffness

Quarry	Asphalt Mixture	Marshall Stability [kN]	S_{MA}	Marshall Stiffness [kN/mm]	MT_{ratio}	Stiffness @ 15°C [MPa]	ITS [MPa]	ITSR
Chlum	Reference ($CaCO_3$)	8.3 7.8	6.0 %	2.40 2.28	0.05	2 495	1.12 1.03	93 %
	BF PKB	6.4 5.5	15.0 %	2.98 1.98	0.34	2 483	1.03 0.78	76 %
	BF Brant	6.4 5.6	12.6 %	2.99 1.97	0.34	2 961	1.07 0.83	78 %
	QD Plešovice	10.1 8.7	13.2 %	4.10 3.23	0.21	5 105	0.99 0.64	65 %
	QD Chrtníky	8.5 8.3	2.0 %	2.81 2.64	0.06	2 667	1.12 1.04	93 %
	QD Litice	8.1 7.4	9.4 %	3.22 2.49	0.23	2 605	1.01 0.69	68 %
	QD Chornice	7.1 4.8	32.7 %	3.20 1.76	0.45	2 813	0.97 0.53	55 %

Strength, durability and stiffness

Quarry	Asphalt Mixture	Marshall Stability [kN]	S_{MA}	Marshall Stiffness [kN/mm]	MT_{ratio}	Stiffness @ 15°C [MPa]	ITS [MPa]	ITSR
Zbečno	Reference ($CaCO_3$)	9.0 6.3	30.3 %	0.41 0.19	0.54	4 566	1.17 0.73	63 %
	BF PKB	9.2 6.5	29.1 %	0.35 0.19	0.45	4 354	1.42 0.91	64 %
	BF Brant	8.1 5.8	28.3 %	0.32 0.16	0.49	4 071	1.38 0.91	66 %
	QD Plešovice	7.5 7.3	2.7 %	0.30 0.23	0.23	4 516	1.25 0.73	59 %
	QD Chrtníky	9.3 9.0	3.6 %	0.40 0.32	0.21	3 646	0.93 1.06	114 %
	QD Litice	9.8 7.6	22.4 %	0.36 0.23	0.37	3 260	1.27 1.08	85 %
	QD Chornice	7.9 5.1	35.6 %	0.24 0.12	0.48	3 766	1.13 0.93	83 %

Artificial Neural Network

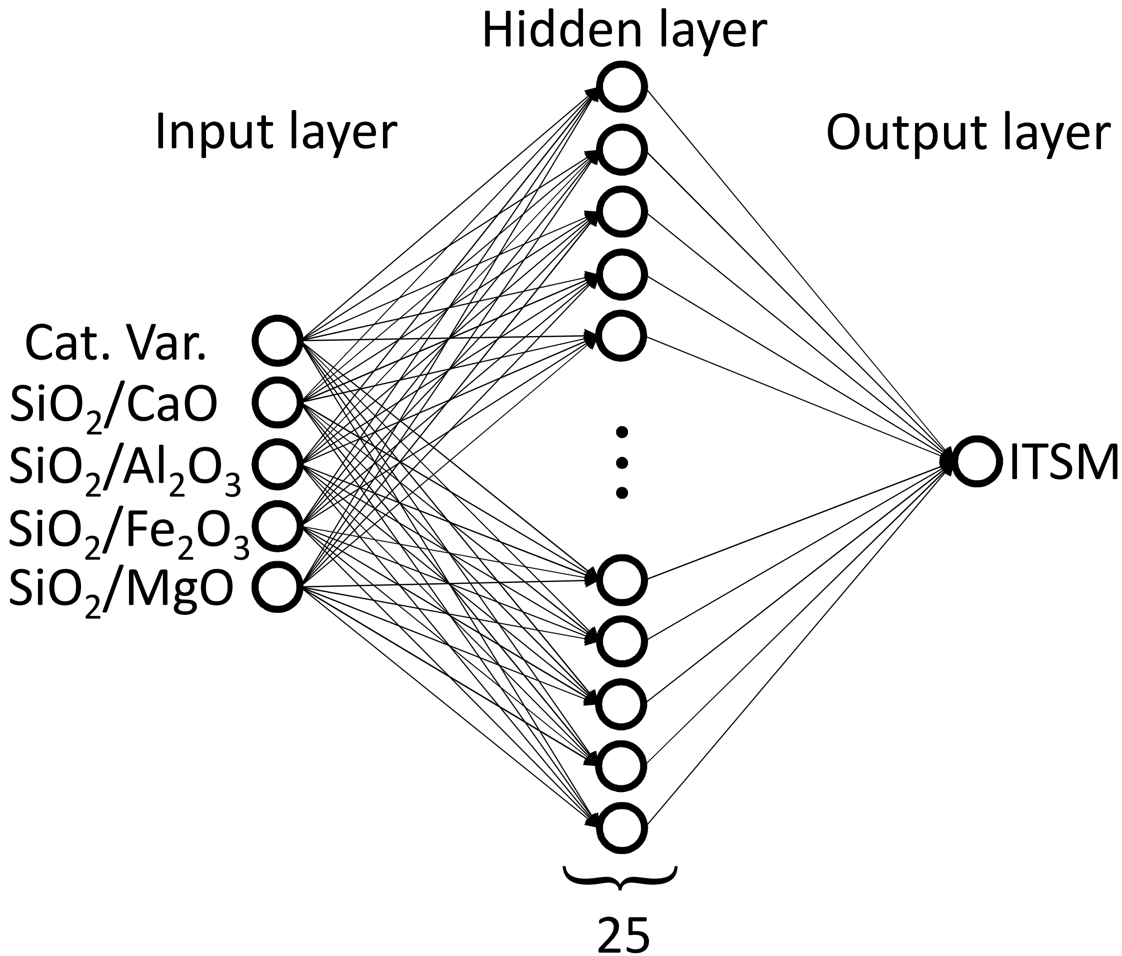

Transfer Function	Equation	Graph
Logistic Sigmoid	$\varphi(x) = \dfrac{1}{1 + e^{-x}}$	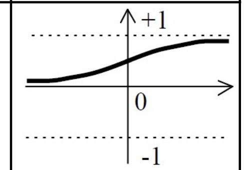
Rectified Linear	$\varphi(x) = \begin{cases} 0 & x < 0 \\ x & x > 0 \end{cases}$	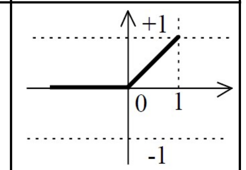
Exponential Linear	$\varphi(x) = \begin{cases} \alpha(e^{x} - 1) & x \leq 0 \\ x & x > 0 \end{cases}$	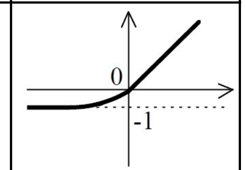
Tangent Sigmoid	$\varphi(x) = \dfrac{e^{x} - e^{-x}}{e^{x} + e^{-x}}$	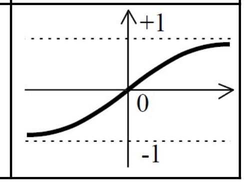

Nicola Baldo
University of Udine

k-fold Cross-Validation

k-fold Cross-Validation is a resampling technique used to elaborate an actual model on a limited data sample. It consists in dividing the data sample in k-partitions. Each sub-sample is used once as validation set and k-1 times as training set. It was decided to give a k-value equal to 6, consistently with the relevant literature.

Iter. 1	Test	Train	Train	Train	Train	Train
Iter. 2	Train	Test	Train	Train	Train	Train
Iter. 3	Train	Train	Test	Train	Train	Train
Iter. 4	Train	Train	Train	Test	Train	Train
Iter. 5	Train	Train	Train	Train	Test	Train
Iter. 6	Train	Train	Train	Train	Train	Test

Results and discussion

The satisfactory results achieved by the different proposed SNNs are expressed by means of the Ordinary Coefficient of Determination (R^2) and the Mean Squared Error (MSE) values. The former represents how the data are well approximated by the regression line: the higher it is, the better the model fits the data. The latter represents the generalizing capabilities of the model through an average of the differences between the experimental investigated modules and those predicted by the SNN squared.

Table 2. Summary Results of the best models.

Inputs	Output	Transfer Function	Best Architecture	R^2	MSE
Cat. Var. SiO_2/CaO SiO_2/Al_2O_3 SiO_2/Fe_2O_3 SiO_2/MgO	ITSM	ELU	5-6-1	0.9372	0.0568
		ReLU	5-12-1	0.9378	0.0538
		TanH	5-5-1	0.9389	0.0572
		LogS	5-4-1	0.9473	0.0445

Results and discussion

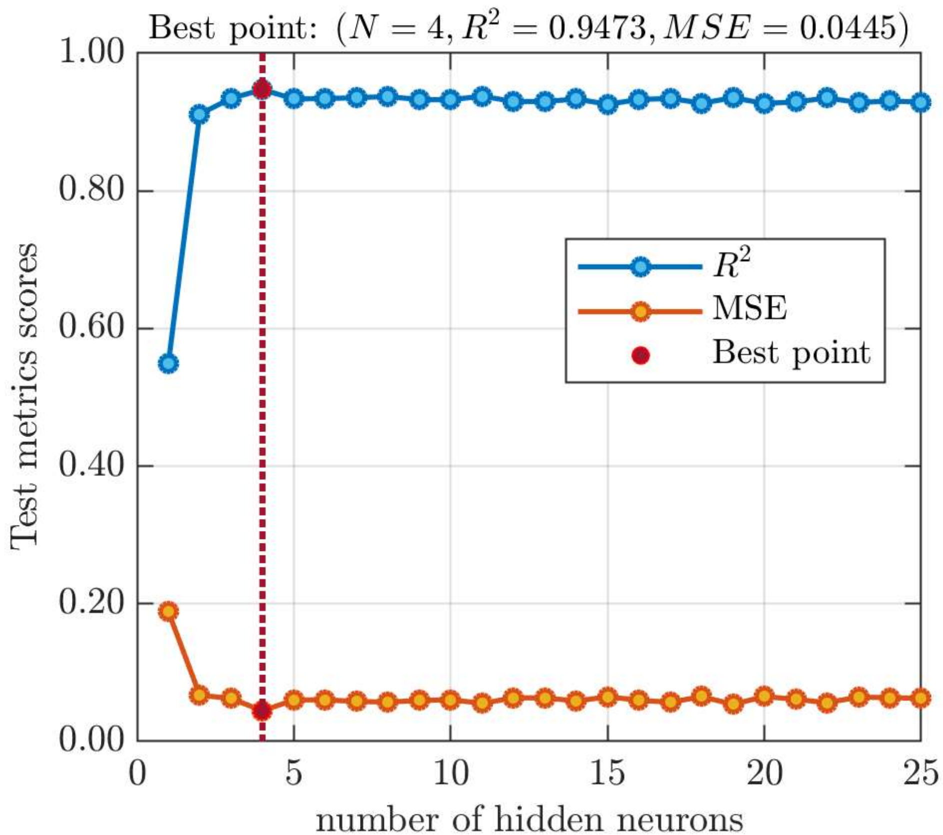

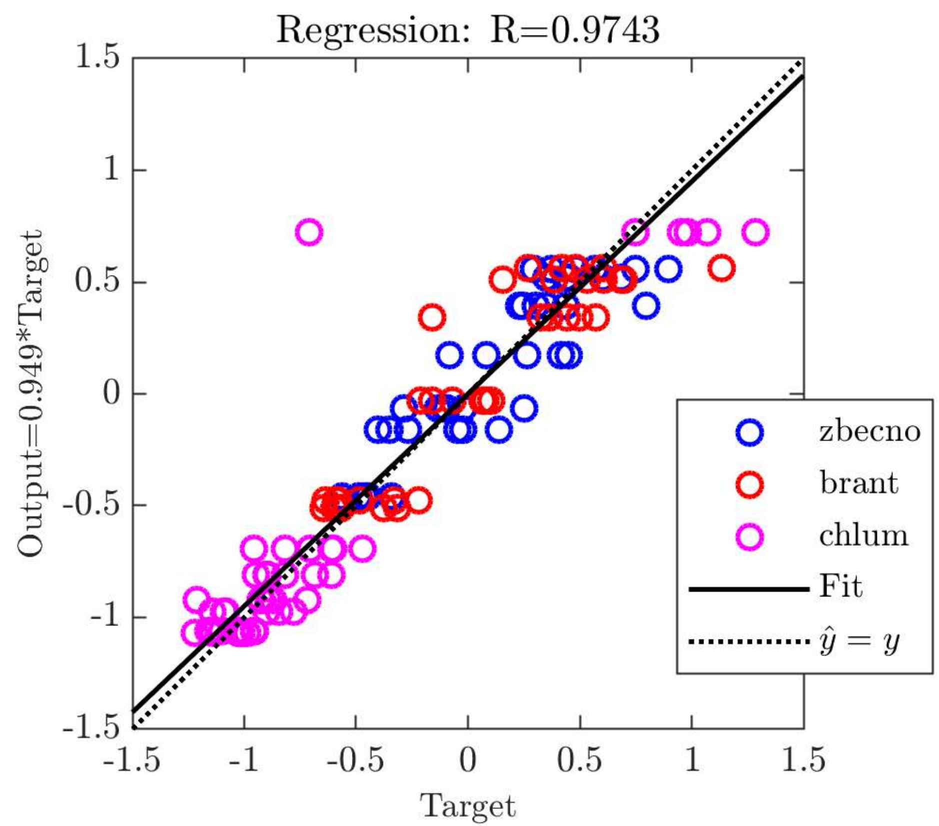

Remarks case study n.3

- An unconventional input type, related to the oxides composition of fillers, along with a categorical variable related to the stone aggregate type, has allowed to properly train neural models aimed to predict stiffness of asphalt concretes, even those made with waste fillers.

- The prediction accuracy of the neural model is resulted good even if only 4 neurons were implemented in the hidden layer.

- Nonlinear transfer functions of different type, require a different number of hidden neurons to achieve the best prediction accuracy.

Case study n.4

sustainability

MDPI

Article

Mechanical Characterization of Industrial Waste Materials as Mineral Fillers in Asphalt Mixes: Integrated Experimental and Machine Learning Analysis

Nitin Tiwari [1,2,*], Nicola Baldo [3,*], Neelima Satyam [2] and Matteo Miani [3]

1 Lyles School of Civil Engineering, Purdue University, West Lafayette, IN 47907, USA
2 Department of Civil Engineering, Indian Institute of Technology Indore, Indore 452020, India; neelima.satyam@iiti.ac.in
3 Polytechnic Department of Engineering and Architecture (DPIA), University of Udine, 33100 Udine, Italy; matteo.miani@phd.units.it
* Correspondence: tiwari50@purdue.edu (N.T.); nicola.baldo@uniud.it (N.B.)

Introduction

This case study regards the feasibility of using seven different materials as alternative filler instead of ordinary Portland cement (OPC) in road pavement base layers, namely **rice husk ash** (RHA), **brick dust** (BD), **marble dust** (MD), **stone dust** (SD), **fly ash** (FA), **limestone dust** (LD), and **silica fume** (SF).

The experimental data were processed through artificial neural networks (ANNs), using k-fold cross validation resampling technique.

Materials and Design

Conventional VG-30 bitumen properties.

Test Parameters	Specified Limit (MoRTH)	Test Results	Test Method
Absolute Viscosity at 60°C, poises	2400-3600	2855	IS 1206 (P-2)
Kinematic Viscosity at 135°C cSt, Min	350	392	IS 1206 (P-3)
Flash point Cleveland open cup, °C, Min	250	304	IS 1448 (P-69)
Penetration at 25°C, 100gm, 5sec, 1/10 mm, Min	45	49	IS 1203
Softening Point (R&B), °C, Min	47	48	IS 1205
Matter Soluble in trichloroethylene, % by mass, Min	99	99.45	IS 1216
Viscosity Ratio at 60°C, Max	4.0	1.3	IS 1206 (P-2)
Ductility at 25°C, cm after TFOT Min	40	75	IS 1208
Specific Gravity gm/cc	0.97 -1.02	0.987	IS 1202

Materials and Design

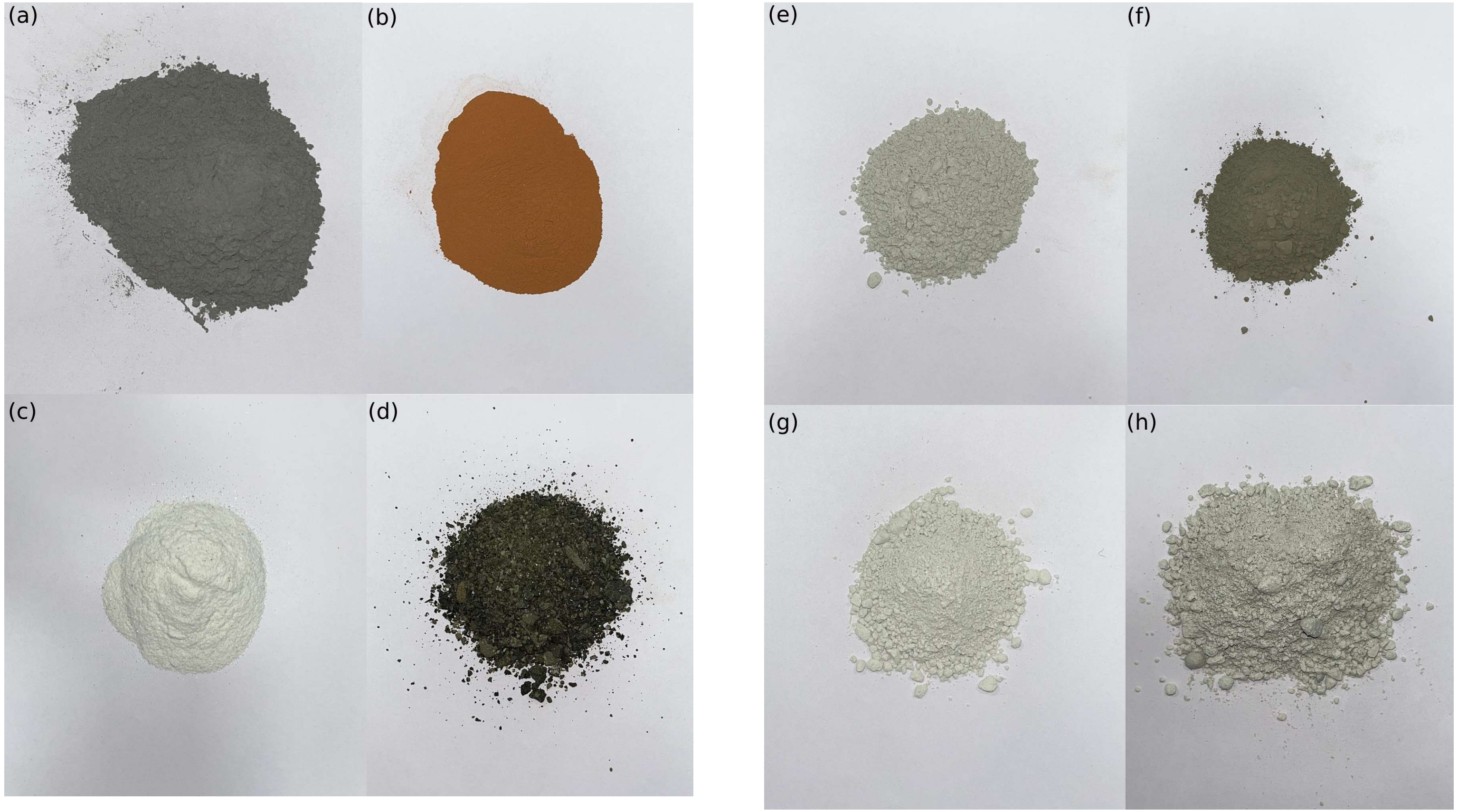

RHA (a), BD (b), MD (c), SD (d), FA (e), OPC (f), LD (g), and SF (h) filler materials.

Materials and Design

Properties of the investigated mineral fillers.

Test parameter	Mineral Filler Type							
	RHA	BD	MD	SD	FA	OPC	LD	SF
Specific gravity (g/cm^3)	2.02	2.56	2.69	2.69	2.32	3.04	2.65	2.20
MBV (g/kg)	4.72	6.25	4.45	3.67	3.86	3.00	3.75	3.85
German filler (g)	65	40	70	85	75	85	97	94
FM	3.21	5.17	2.12	5.38	3.77	4.96	3.03	1.96
Surface area (m^2/g)	2.31	2.69	4.37	2.70	2.19	1.75	2.70	16.45
PH	10.86	8.67	8.50	12.57	7.30	12.90	10.22	6.98
SiO_2 (%)	89.67	39.55	0.60	82.37	48.24	21.43	0.48	93.5
CaO (%)	1.88	12.88	55.60	2.79	13.40	66.58	96.57	0.89
Al_2O_3 (%)	1.62	15.71	0.40	8.23	24.15	3.01	0.41	0.08
MgO (%)	0.97	3.29	0.10	1.47	1.46	1.39	0.46	0.82
Fe_2O_3 (%)	1.06	14.05	0.20	5.27	6.48	4.68	0.32	0.50
Particle shape	Honeycombed	Subangular particles	Subangular particles	Angular particles	Rounded	Granular/ subangular particles	Granular particles	Spherically shaped

Materials and Design

Crushed quartz aggregate properties

Test Parameters	Specified Limit (MoRTH)	Test Results	Test Method
Cleanliness (Dust) (%)	Max 5 %	3	IS 2386 Part I
Bulk Specific gravity (g/cm3)	2-3	2.68	IS 2386 Part III
Percent wear by Los Angeles abrasion (%)	Max 35 %	10.6	IS 2386 Part IV
Soundness loss by sodium sulphate solution (%)	Max 12%	3.4	IS 2386 Part V
Soundness loss by magnesium sulphate solution (%)	Max 18%	3.7	IS 2386 Part V
Flakiness and Elongation Index (%)	Max 35%		IS 2386 Part I
– 20 mm		27.93	
– 10 mm		32.13	
Impact Strength (%)	Max 27%		IS 2386 Part IV
– 20 mm		4.15	
– 10 mm		5.91	
Water Absorption (%)	Max 2%	1.67	IS 2386 Part III

Materials and Design

Aggregate type, grain size distribution, and bitumen type have been kept constant for all the asphalt concretes investigated in order to assess only the effect of the different filler materials on the physical-mechanical response of the mixes.

Four levels of waste mineral filler have been considered, namely, 4.0%, 5.5%, 7.0%, and 8.5%, by volume of mix; OPC has been used with the same contents as a comparative term.

Marshall compaction and stability, Indirect Tensile Strenght, Cantabro Abrasion Loss, modified Lottman test.

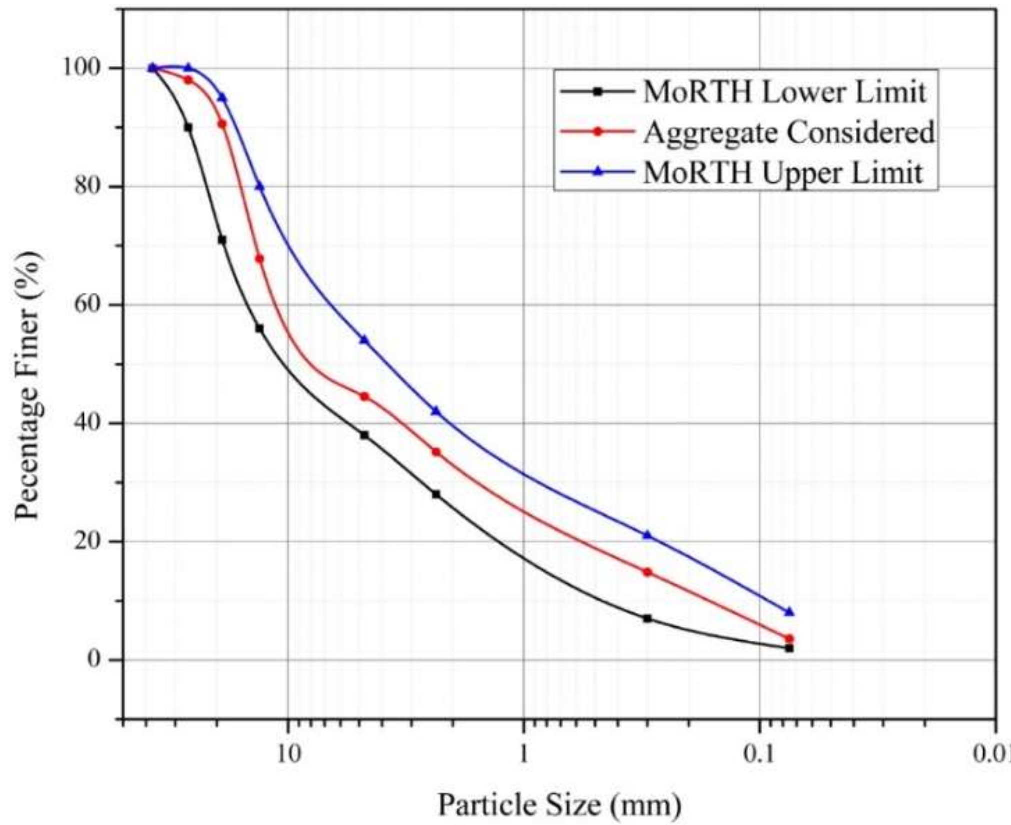

Design gradation curve and MoRTH limits.

Results and discussion

VOLUMETRIC PROPERTIES

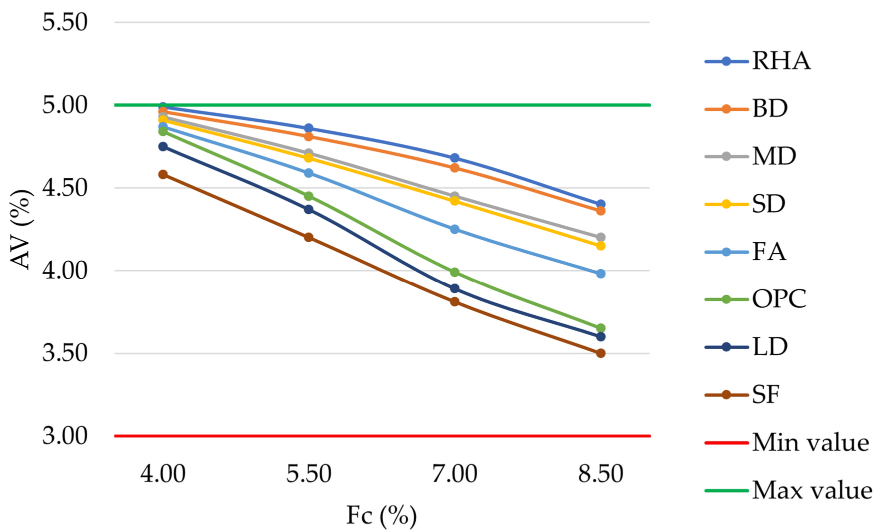

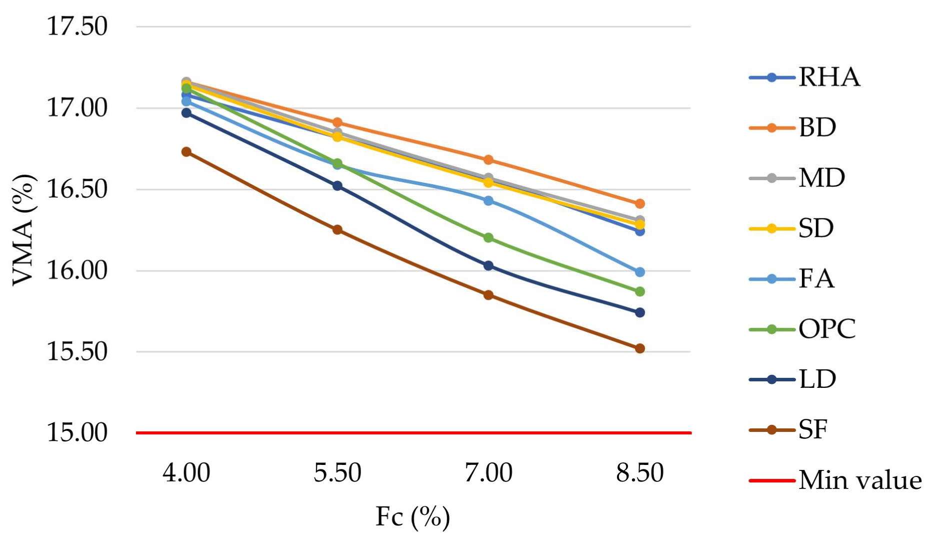

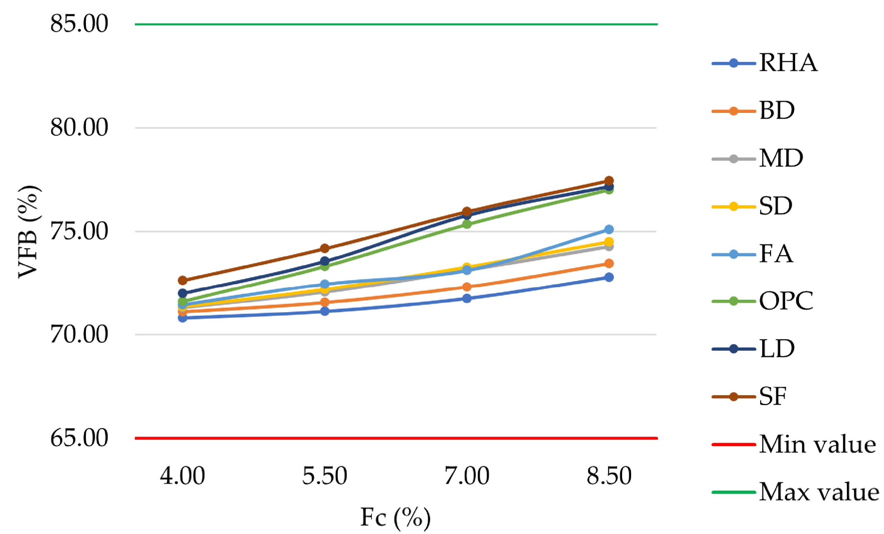

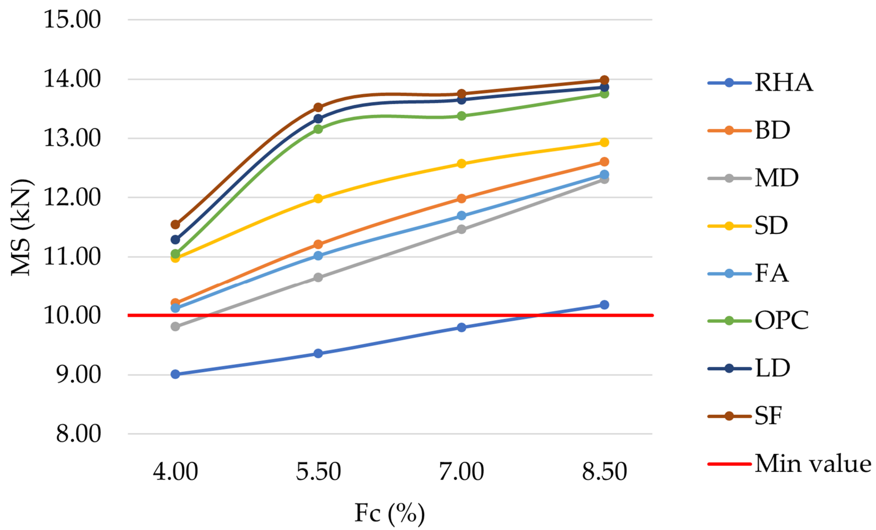

Results and discussion

MARSHALL PARAMETERS and CANTABRO LOSS

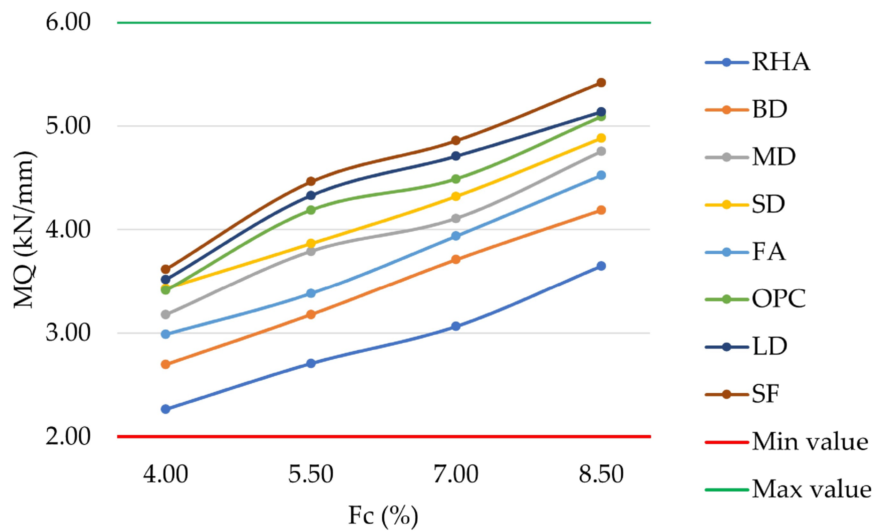

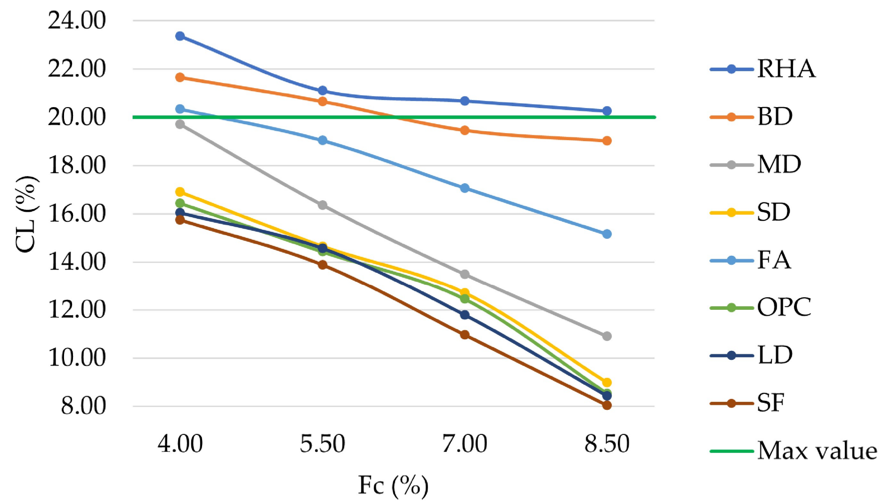

Results and discussion

INDIRECT TENSILE STRENGTH

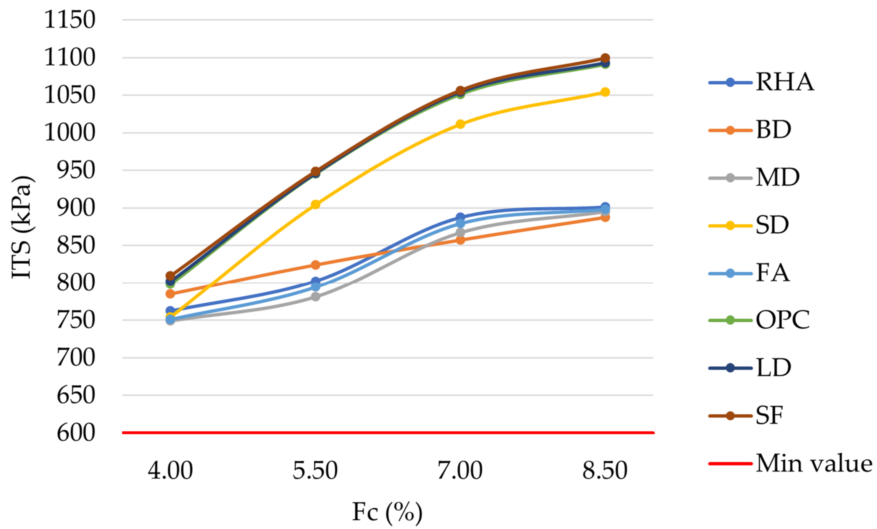

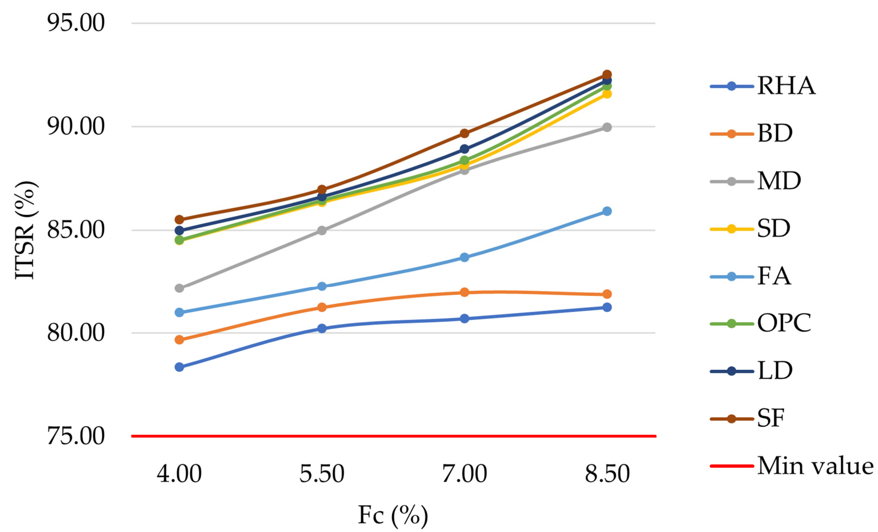

Artificial Neuron

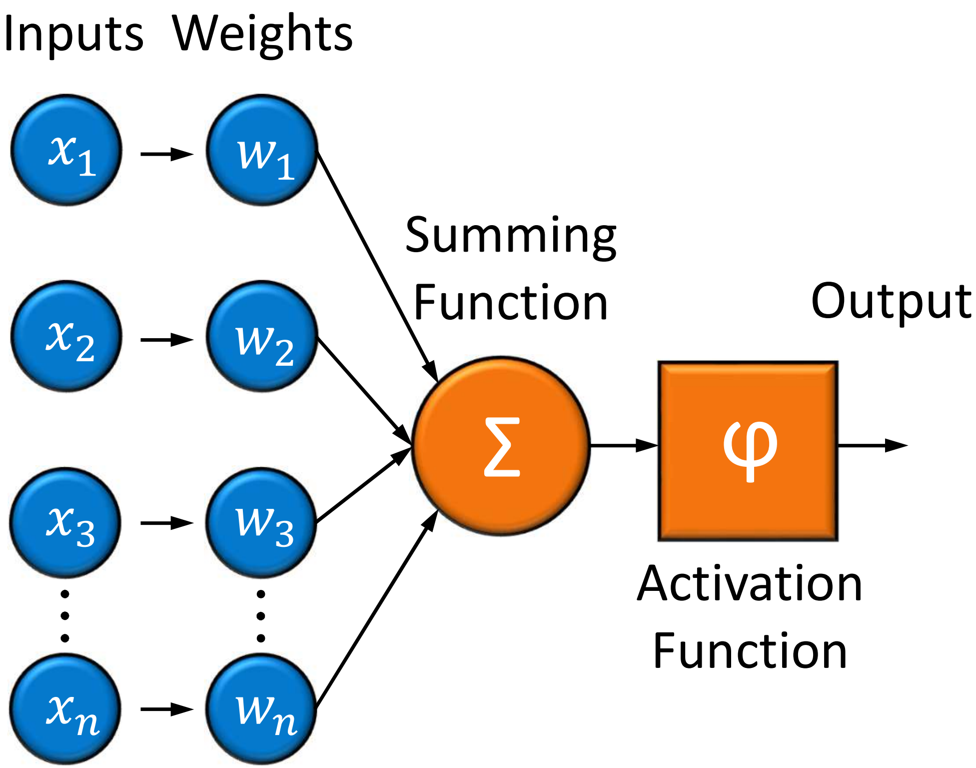

Activation functions investigated

Activation Function	Equation	Graph
Exponential Linear	$\varphi(x) = \begin{cases} \alpha(e^x - 1) & x \leq 0 \\ x & x > 0 \end{cases}$	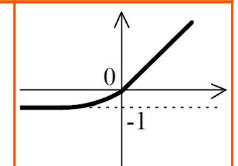
Hyperbolic Tangent	$\varphi(x) = \dfrac{e^x - e^{-x}}{e^x + e^{-x}}$	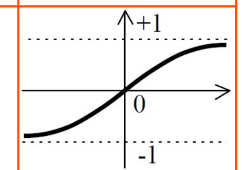

Neural Modeling

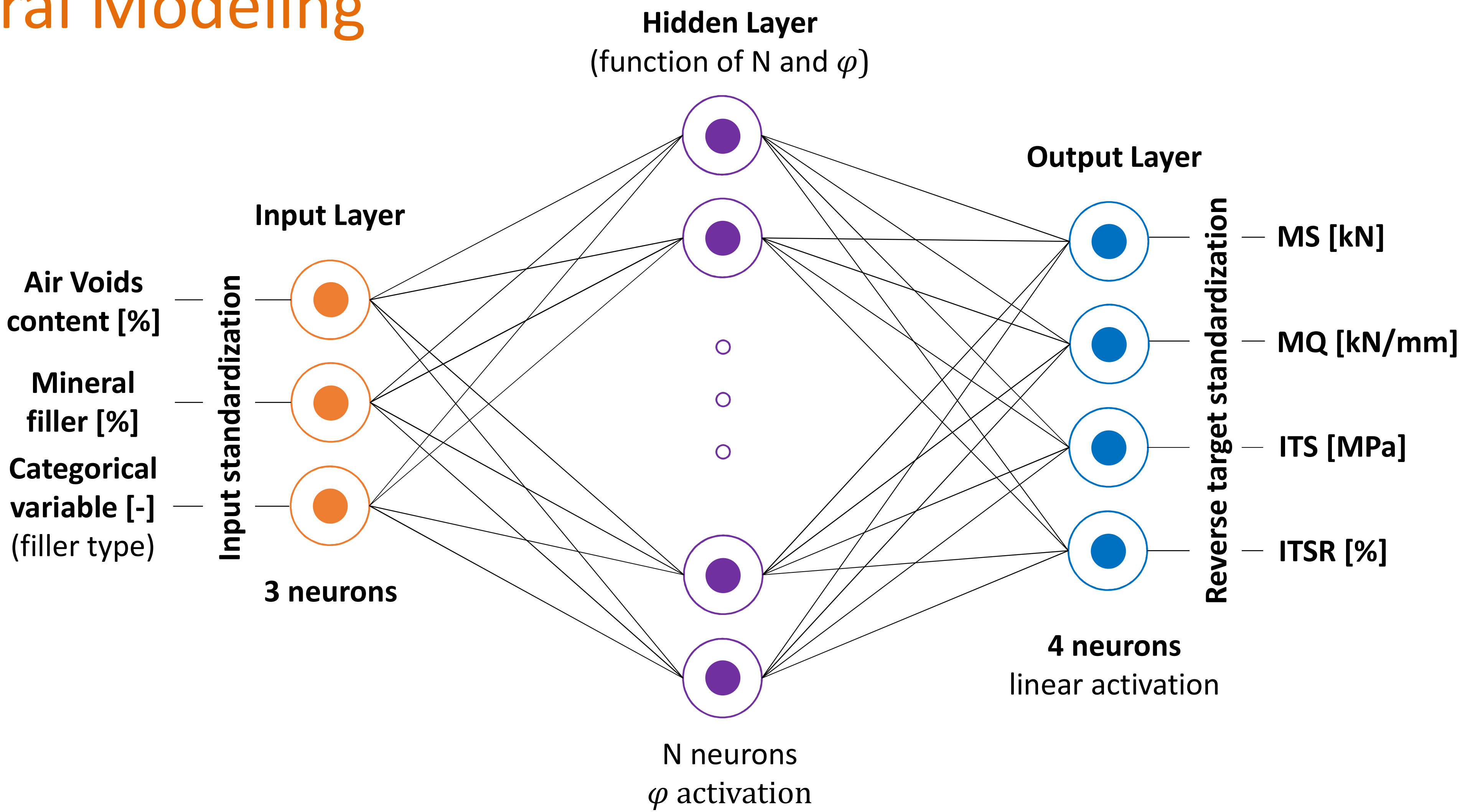

k-fold Cross-Validation

Randomly mix the dataset

↓

Split the dataset into k = 4 folds

↓

	Fold 1	Fold 2	Fold 3	Fold 4	
Iteration 1	Validation	Train	Train	Train	Validation score 1
Iteration 2	Train	Validation	Train	Train	Validation score 2
Iteration 3	Train	Train	Validation	Train	Validation score 3
Iteration 4	Train	Train	Train	Validation	Validation score 4

↓

Average the scores obtaining the general performance of the model

Training Process

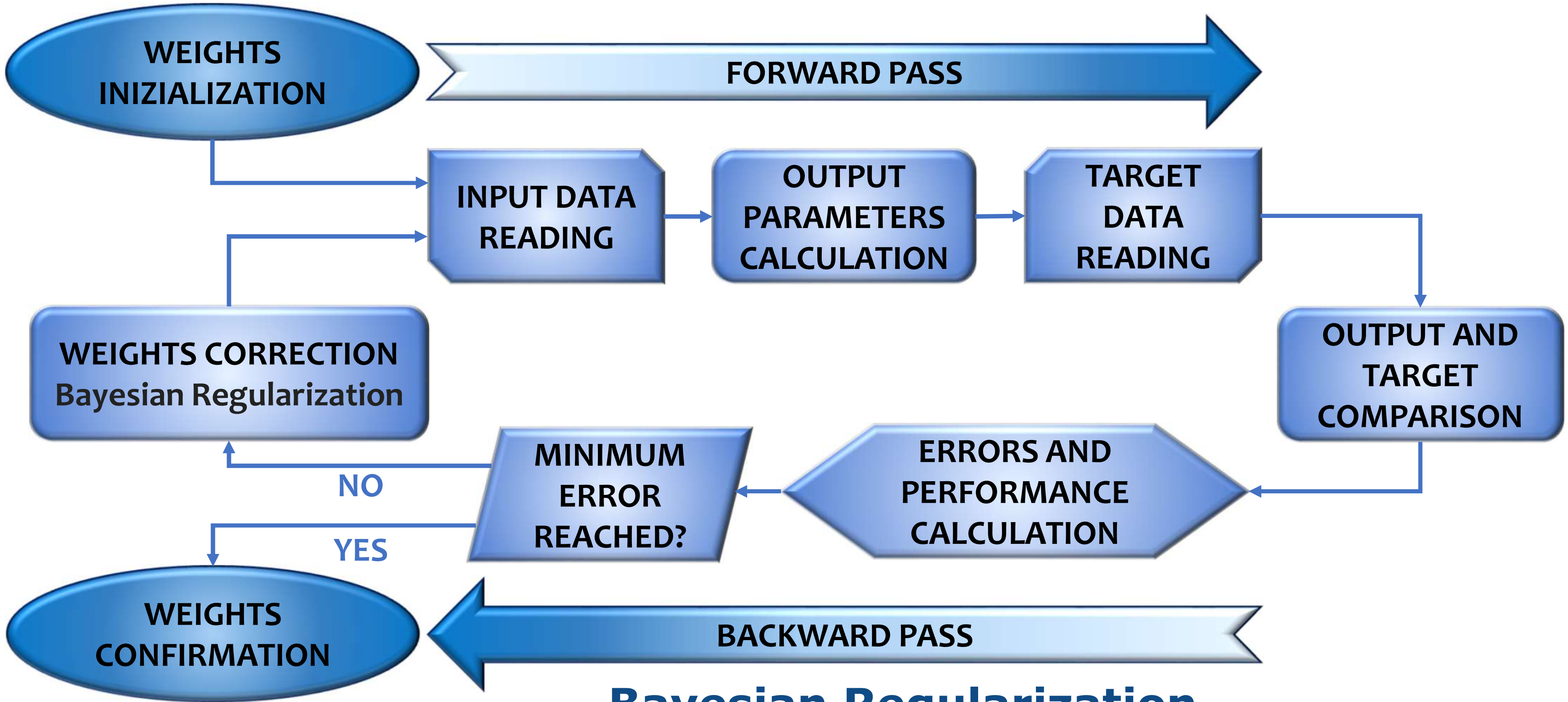

Bayesian Regularization

Data Augmentation

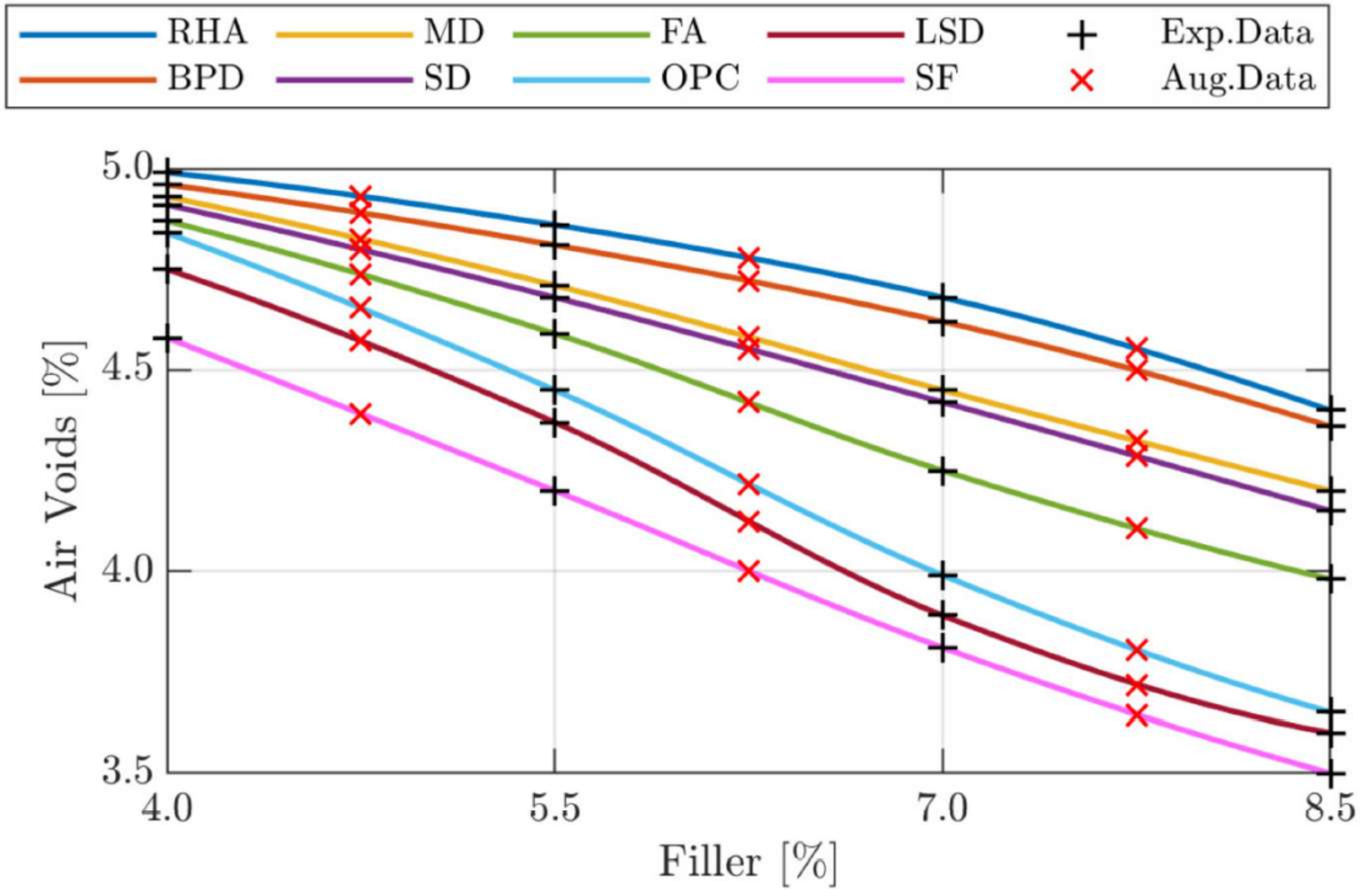

Augmented points (red cross marker) and available experimental points functions (black plus sign marker).

- Synthetic data generation
- Unaltered collected information meaning

Makima Interpolation

$$z(x,y) = \sum_{j=0}^{3} \sum_{k=0}^{3-j} q_{jk} x^j y^k$$

Neural Modeling Results

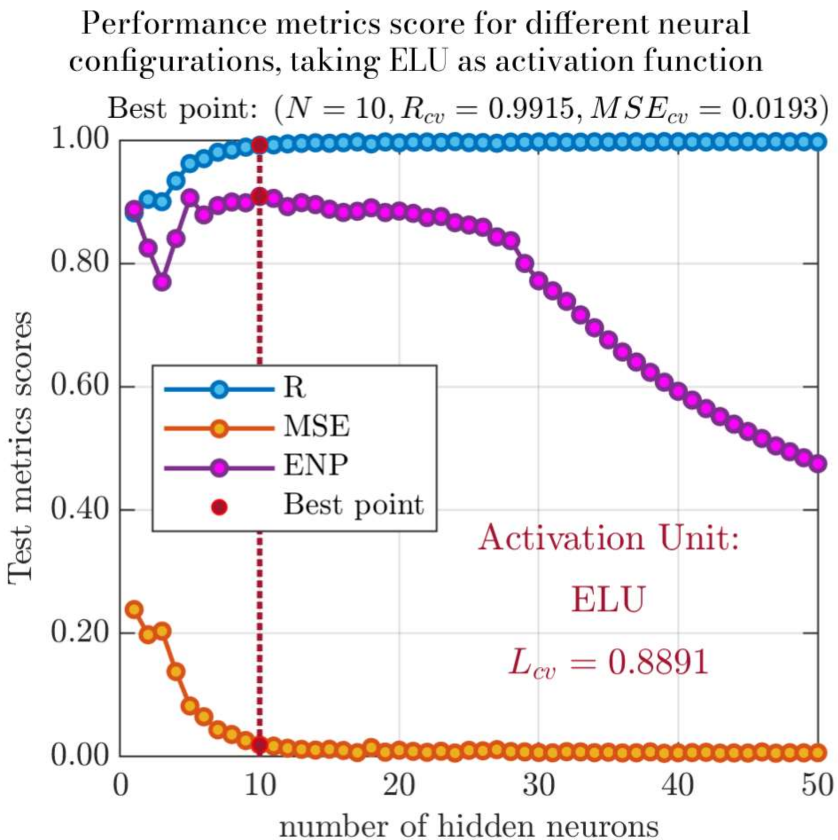

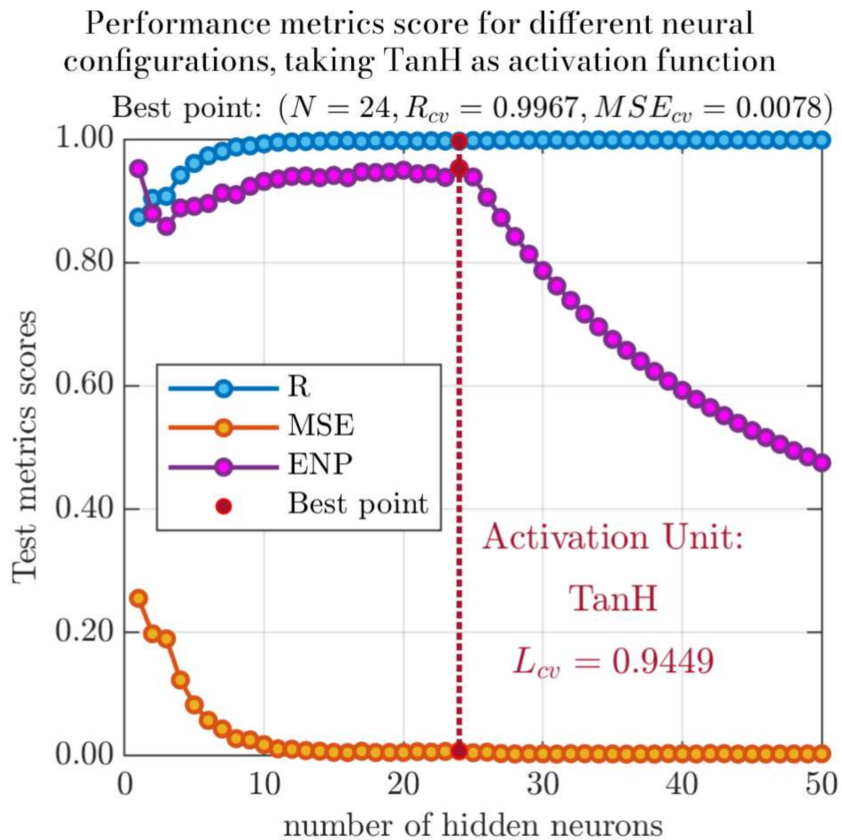

Remarks case study n.4

- WASTE Fillers can replace conventional filler in asphalt concretes.

- k-folds resampling and MAKIMA data-augmentation methods allow to properly train neural models.

- The Artificial Neural Network architecture should be always optimized.

Case study n.5

sustainability

MDPI

Article

Foamed Bitumen Mixtures for Road Construction Made with 100% Waste Materials: A Laboratory Study

Nicola Baldo [1,*], Fabio Rondinella [1,*], Fabiola Daneluz [1] and Marco Pasetto [2]

1 Polytechnic Department of Engineering and Architecture (DPIA), University of Udine, Via del Cotonificio 114, 33100 Udine, Italy; fabiola.daneluz@uniud.it
2 Department of Civil, Environmental and Architectural Engineering (DICEA), University of Padua, Via Marzolo 9, 35131 Padua, Italy; marco.pasetto@unipd.it
* Correspondence: nicola.baldo@uniud.it (N.B.); fabio.rondinella@phd.units.it (F.R.)

Waste Materials

Electric Arc Furnace (EAF) steel slags

Municipal Solid Waste Incineration (MSWI) bottom ash

Glass Waste (GW)

Ladle Furnace (LF) slags

Coal Fly (CF) ash

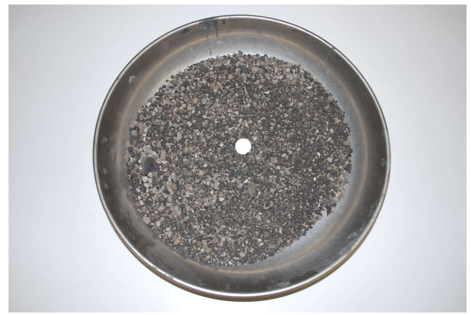

RAP

Initial concentration of major heavy metals

Element	Initial Concentration (mg/kg)				
	EAF Slags	LF Slags	MSWI Ash	CF Ash	GW
Copper (Cu)	188.9	107.0	575.0	304.6	989.0
Cadmium (Cd)	14.5	<0.5	1.2	2.3	<0.5
Lead (Pb)	58.2	7.1	480.0	54.8	226.0
Zinc (Zn)	749.2	63.3	815.0	217.4	901.0
Chromium, Total (Cr)	18,150.5	599.0	60.0	292.7	250
Chromium, Hexavalent (Cr)	<1	<5.0	<0.1	1.8	<5
Nickel (Ni)	74.1	27.6	55.0	143.8	13.8
Mercury (Hg)	1.0	<0.5	<0.1	<1.0	<0.5
Selenium (Se)	87.3	5.3	<0.1	62.7	<2.0
Arsenic (As)	131.5	14.7	<0.1	23.7	<2.0
Beryllium (Be)	0.5	0.6	<0.1	4.5	0.9
Antimony (Sb)	6.0	7.3	2.9	5.6	2.0
Thallium (Tl)	19.1	<0.5	<0.01	<1.0	<0.5

Leaching concentration of major heavy metals

Element	UM	TCLP Leaching Concentration					
		EAF Slags	LF Slags	MSWI Ash	CF Ash	GW	Legal Threshold
Copper (Cu)	(mg/L)	<0.001	0.001	0.042	<0.05	0.043	<0.05
Cadmium (Cd)	(µg/L)	<1.0	<1.0	<0.3	<5.0	<1.0	<5
Lead (Pb)	(µg/L)	<5.0	10.7	15.0	<50.0	<5.0	<50
Zinc (Zn)	(mg/L)	0.004	<0.001	0.018	<3.0	<0.001	<3
Chromium (Cr)	(µg/L)	38.0	1.3	23.0	<50.0	<1.0	<50
Nickel (Ni)	(µg/L)	<3.0	<3.0	0.6	<10.0	<3.0	<10
Mercury (Hg)	(µg/L)	<1.0	<1.0	0.2	<1.0	<1.0	<1
Selenium (Se)	(µg/L)	<5.0	<5.0	1.7	<10.0	<5.0	<10
Arsenic (As)	(µg/L)	<5.0	<5.0	<2.0	<50.0	<5.0	<50
Barium (Ba)	(mg/L)	0.5	0.002	0.85	<1.0	0.01	<1

Physical and mechanical characteristics of waste materials

Properties	Reference Standards	EAF Slags	LF Slags	MSWI Ash	CF Ash	GW	RAP
Equivalent in sand (%)	EN 933-8	79	52	65	–	68	82
Shape Index (%)	EN 933-4	2	5	6	–	14	10
Flakening Index (%)	EN 933-3	5	2	9	–	32	7
Los Angeles coefficient (%)	EN 1097-2	19	–	–	–	–	27
Particle density (Mg/m^3)	EN 1097-6	3.71	2.23	2.21	2.01	2.45	2.36

Waste materials grading curves

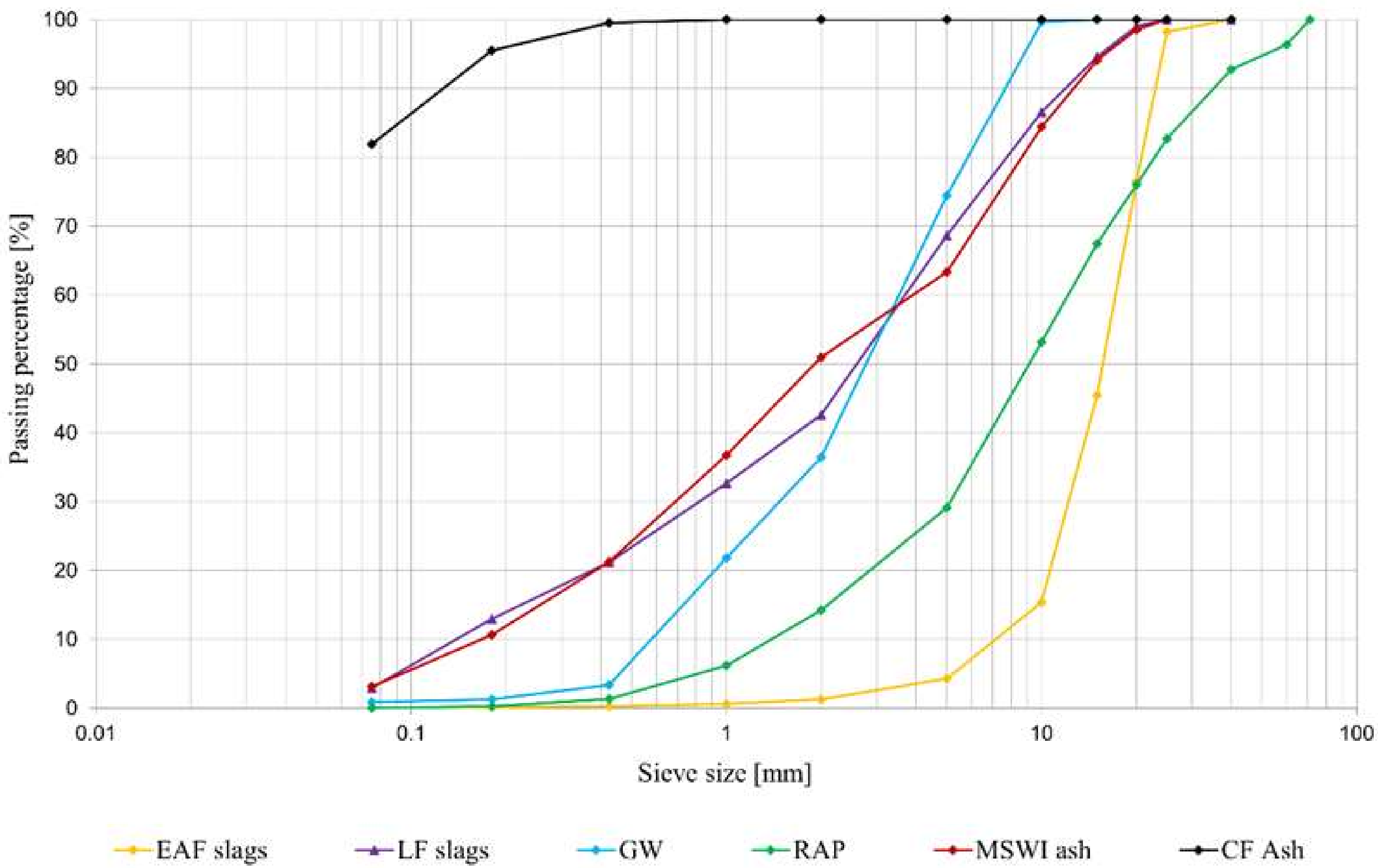

Limestone aggregates grading curves

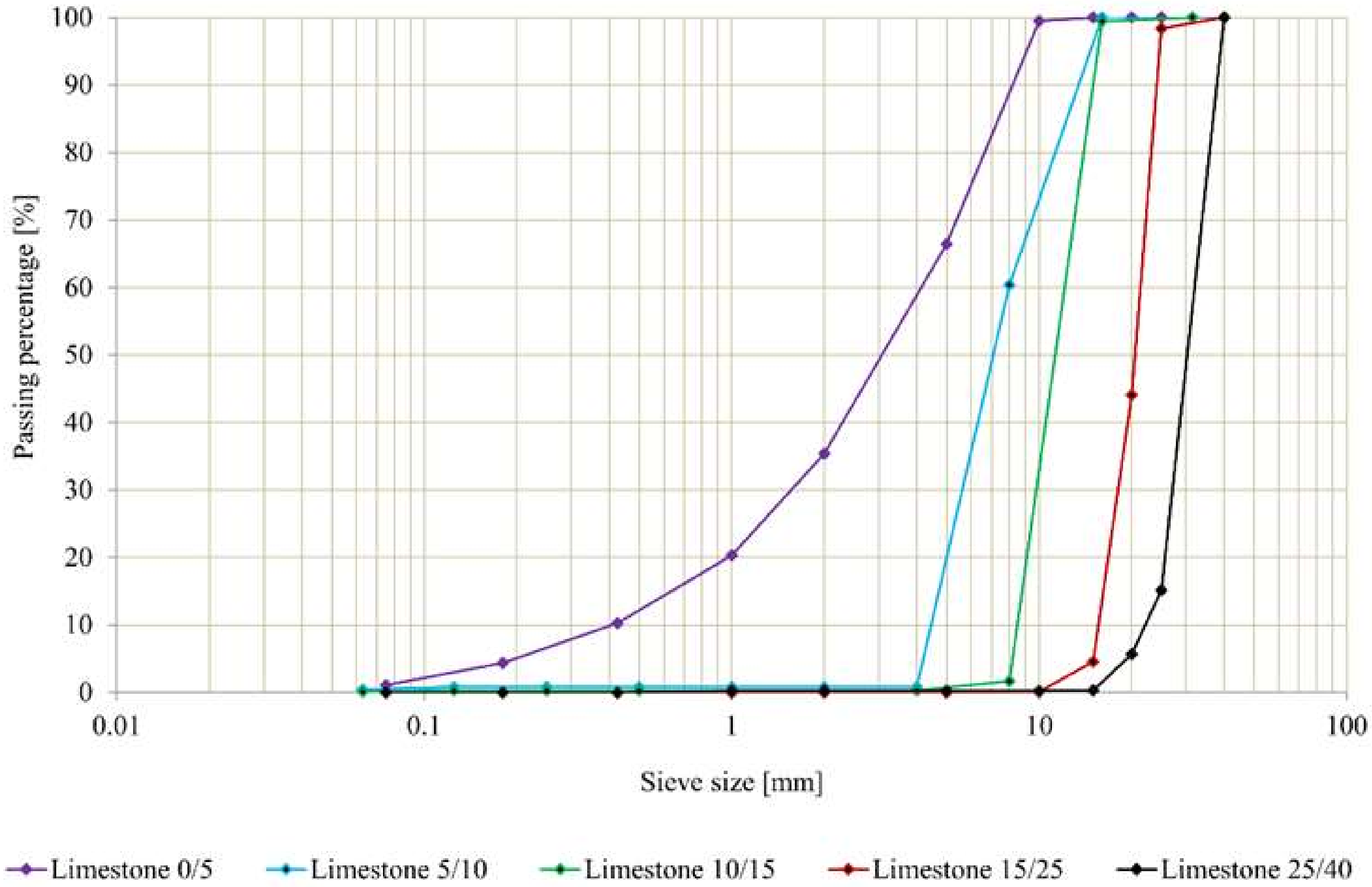

Mixtures composition (%)

Aggregate Type	Mix 1	Mix 2	Mix 3	Mix 4	Mix 5	LS
EAF slags	20	20	20	20	20	0
LF slags	10	10	10	10	10	0
MSWI ash	0	10	20	30	40	0
CF ash	10	10	10	10	10	0
GW	40	30	20	10	0	0
RAP	20	20	20	20	20	0
Limestone 0/5	0	0	0	0	0	40
Limestone 5/10	0	0	0	0	0	15
Limestone 10/15	0	0	0	0	0	15
Limestone 15/25	0	0	0	0	0	12
Limestone 25/40	0	0	0	0	0	10
Filler	0	0	0	0	0	8

Design grading curves of the mixtures

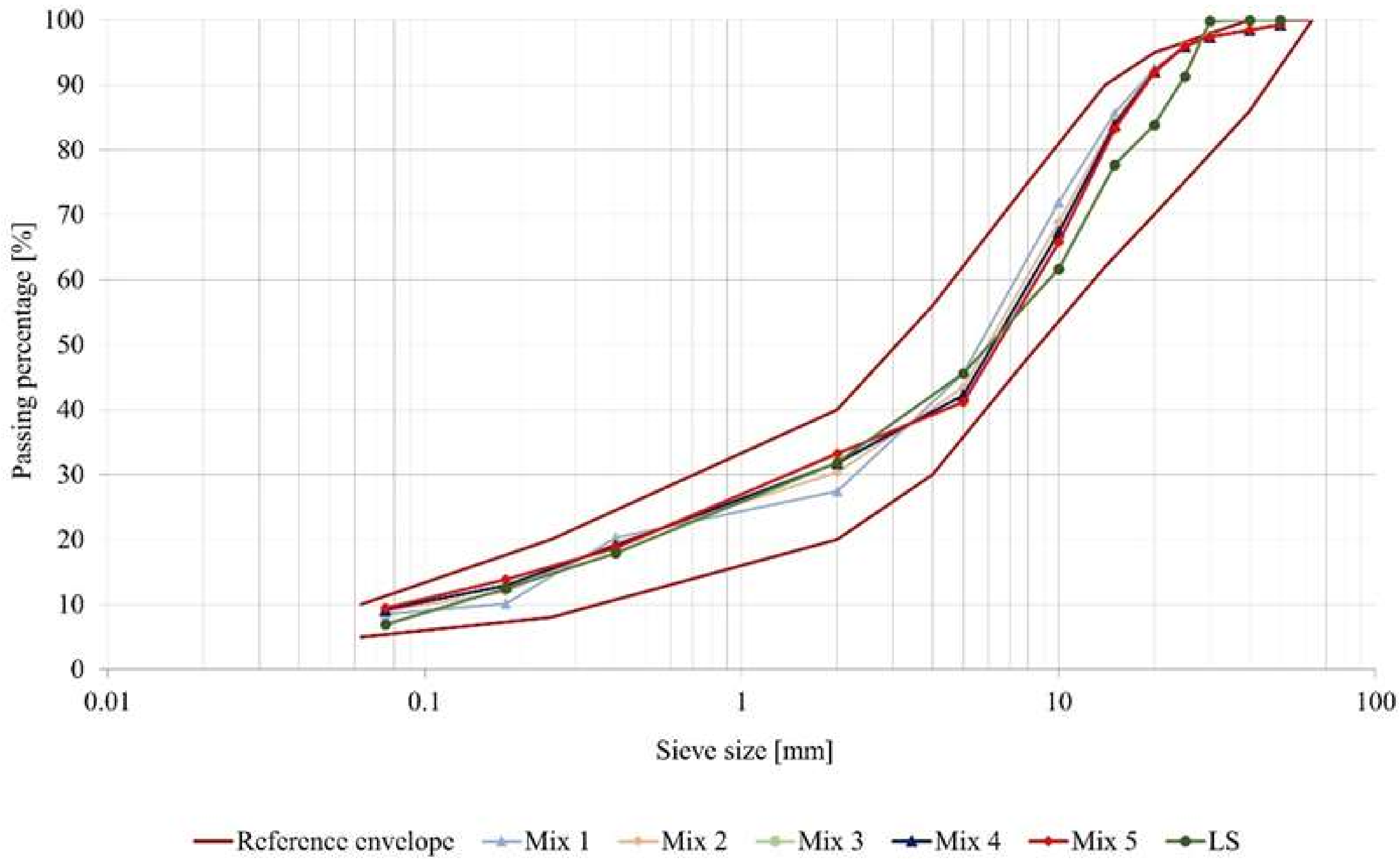

Materials: bitumen

"soft" bitumen, 80/100 penetration grade

(82 dmm at 25 ° C)

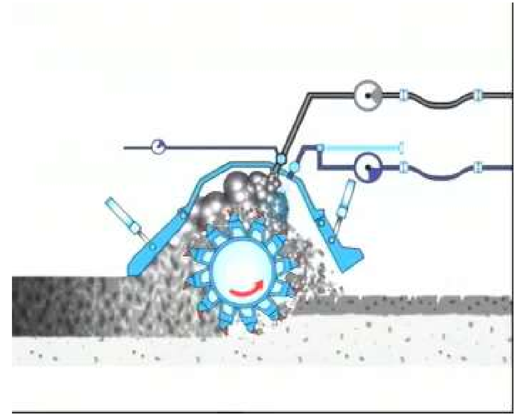

Cold recycling

Foam collapse

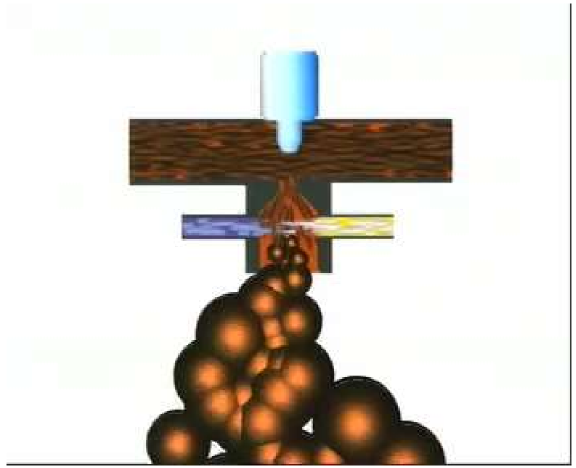

Expansion chamber

Laboratory foaming equipment

Foamed bitumen mixtures vs Hot Mix Asphalt

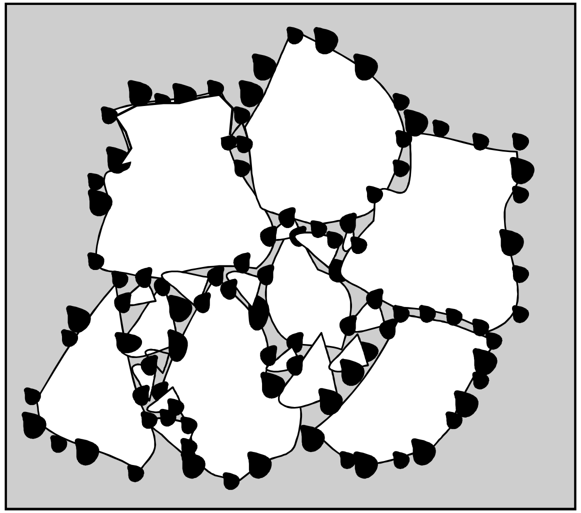

Bitumen "Spot Welds" between Aggregate Particles

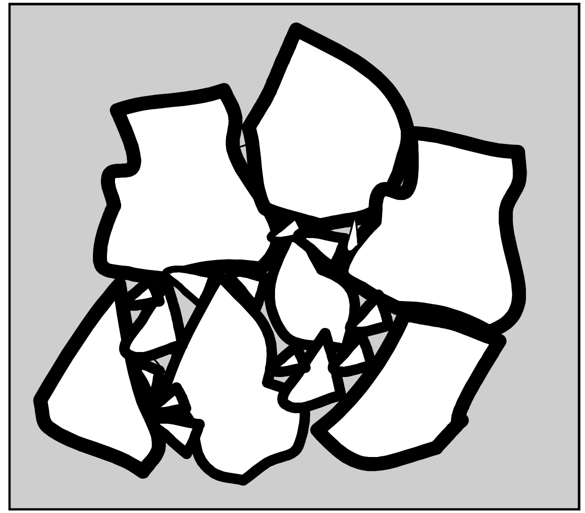

Conventional bitumen film coating of aggregate particles

Indirect Tensile Strength (ITS)

EN 12697-23

Curing conditions

- ✓ 24 h in the mould, at room temperature
- ✓ 72 h at 40° C

Test conditions

- ✓ Temperature: 25° C
- ✓ Strain rate: 0.85 mm/s
- ✓ Dry/Wet conditions
- ✓ Soaked samples: 24 h in water at 25° C

Indirect Tensile Stiffness Modulus

EN 12697/26 - Annex C

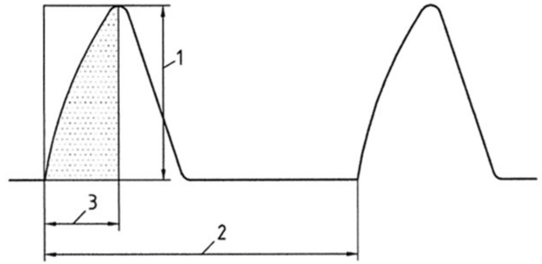

$$S_m = \frac{F(\nu + 0.27)}{z \cdot h}$$

Test conditions

- ✓ Temperature: 25° C
- ✓ Rise Time: 124 ms
- ✓ Strain amplitude: 5 microns
- ✓ 2 diameters
- ✓ 10 conditioning pulses

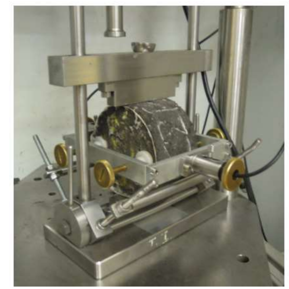

Test results (@ 2% cement & 2% Foamed bitumen)

Aggregate Type	Mix 1	Mix 2	Mix 3	Mix 4	Mix 5	LS
ITS dry (MPa)	0.54	0.57	**0.62**	0.49	0.40	0.28
ITS soaked (MPa)	0.38	0.42	**0.47**	0.33	0.26	0.17
TSR (%)	0.70	0.74	**0.76**	0.67	0.65	0.61

MatLab Neural Network Fitting Toolbox

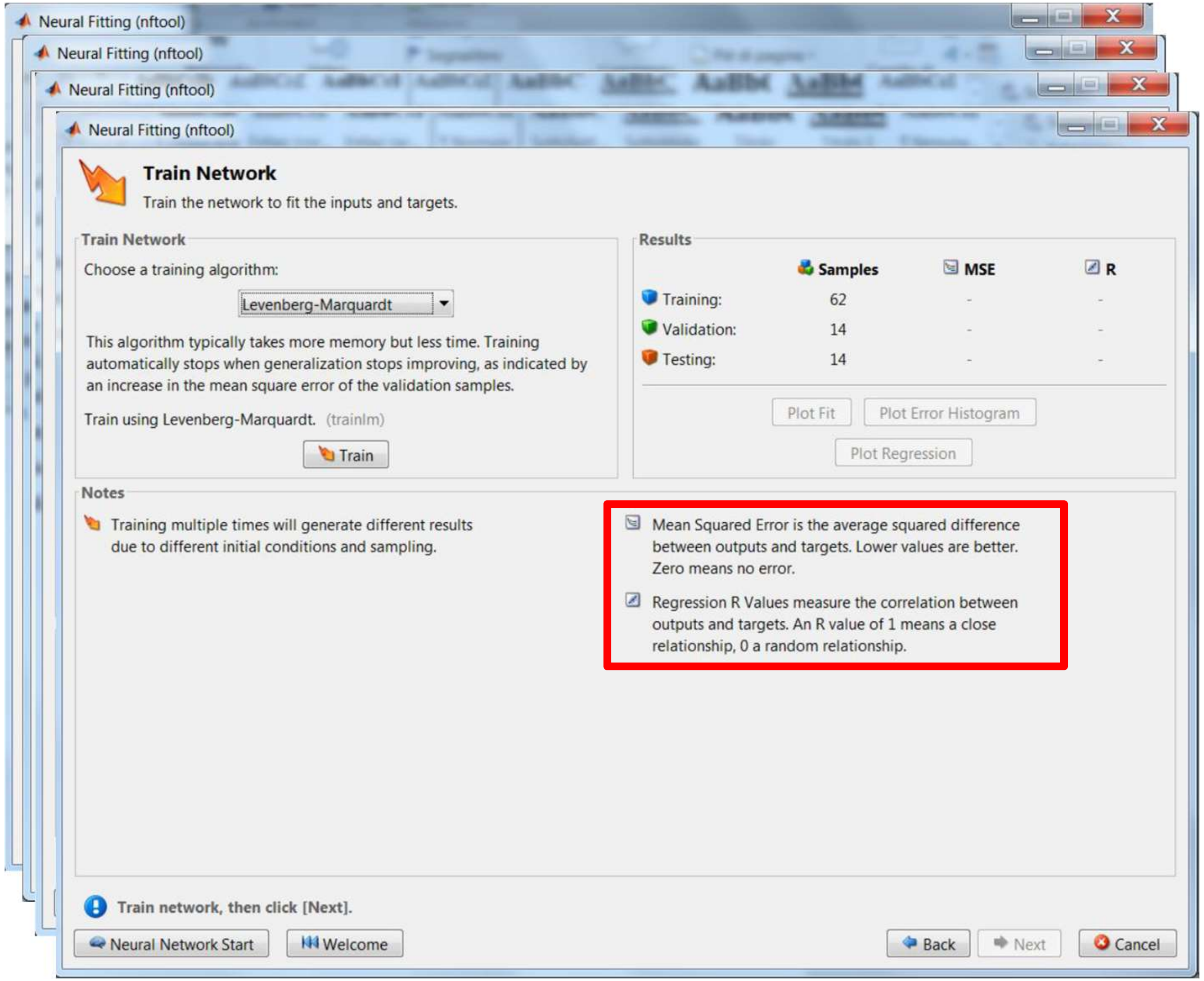

Data Set sampling

Training: 70%

Validation: 15%

Testing: 15%

$$MSE = \frac{\sum_{i=1}^{n}(y_i - t_i)^2}{n}$$

$$R = \frac{\sum_{i=1}^{n}(y_i - \hat{y})(t_i - \hat{t})}{\sqrt{\sum_{i=1}^{n}(y_i - \hat{y})^2 \sum_{i=1}^{n}(t_i - \hat{t})^2}}$$

Neural modeling

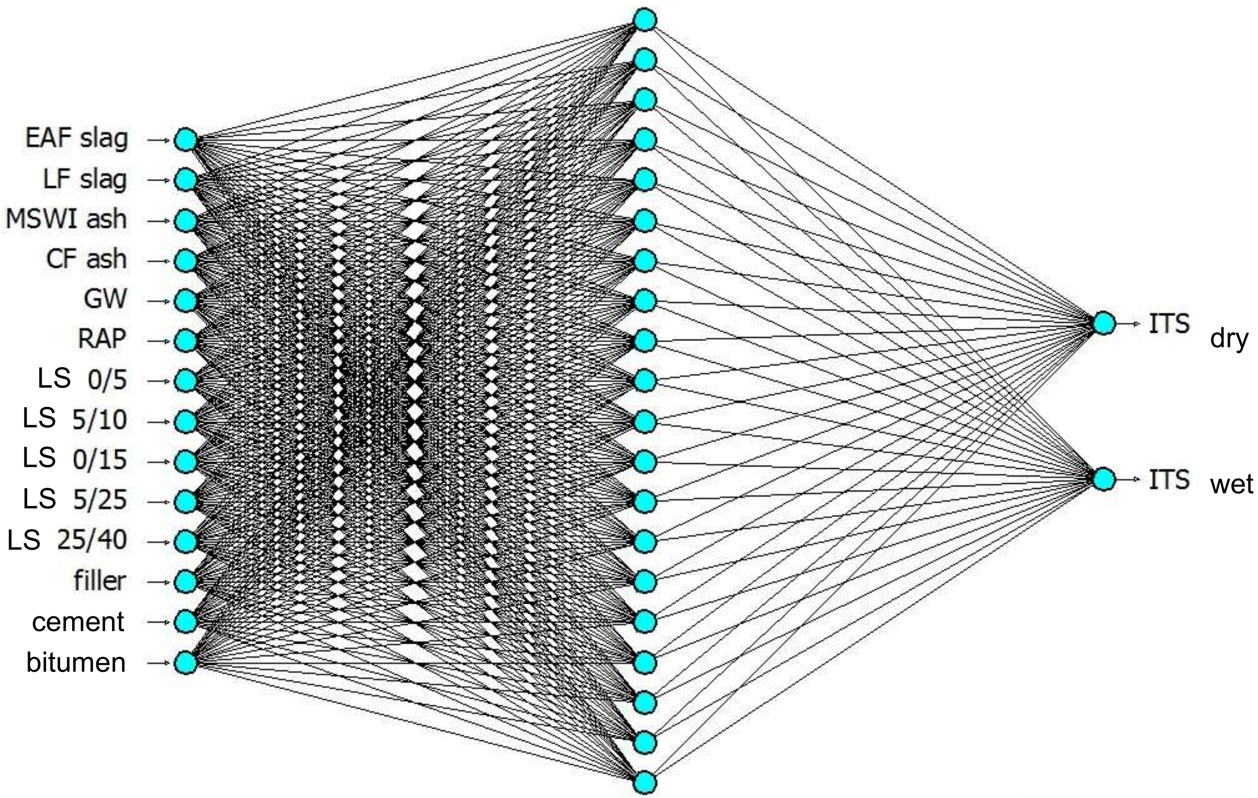

Activation Function	Equation	Graph
Linear	$\varphi(x) = x$	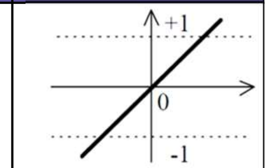
Hyperbolic Tangent	$\varphi(x) = \dfrac{e^{x} - e^{-x}}{e^{x} + e^{-x}}$	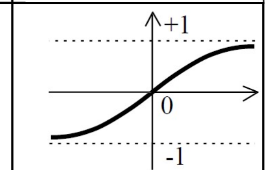
Logistic Sigmoid	$\varphi(x) = \dfrac{1}{1 + e^{-x}}$	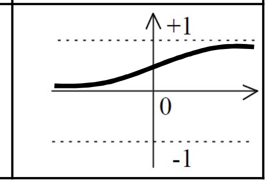

Modeling results

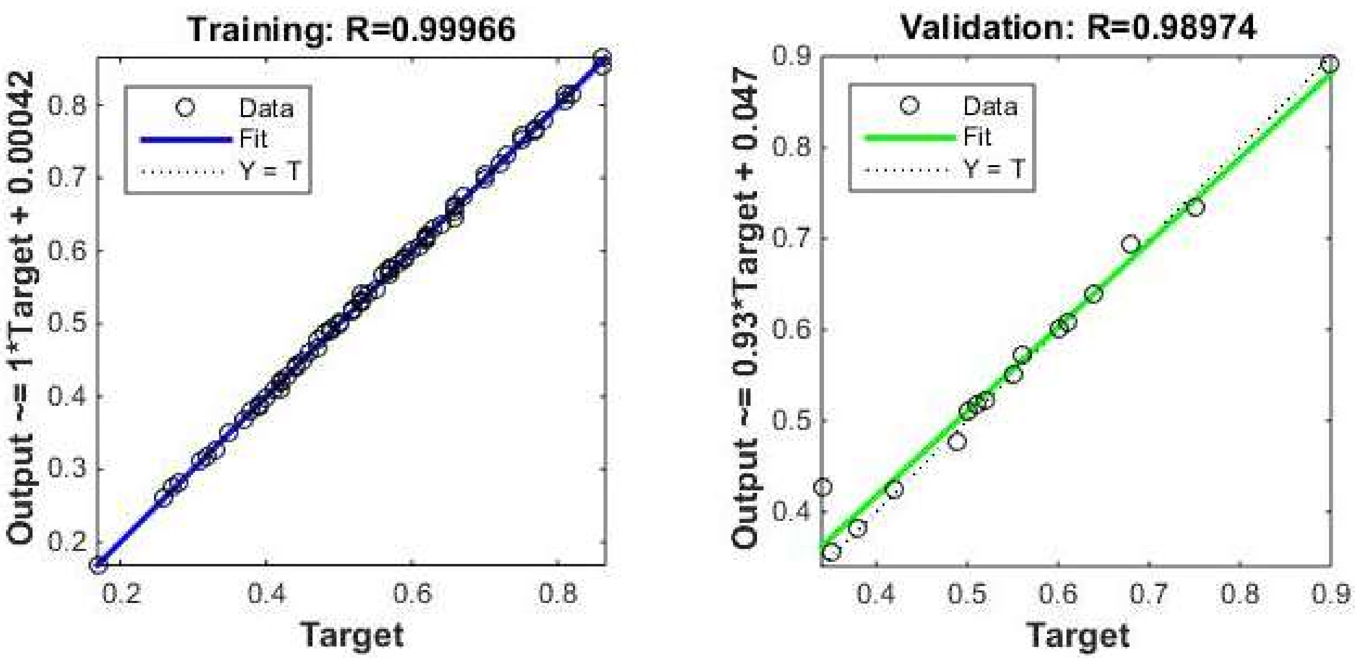

Dry ITS (ANN output vs Experimental data)

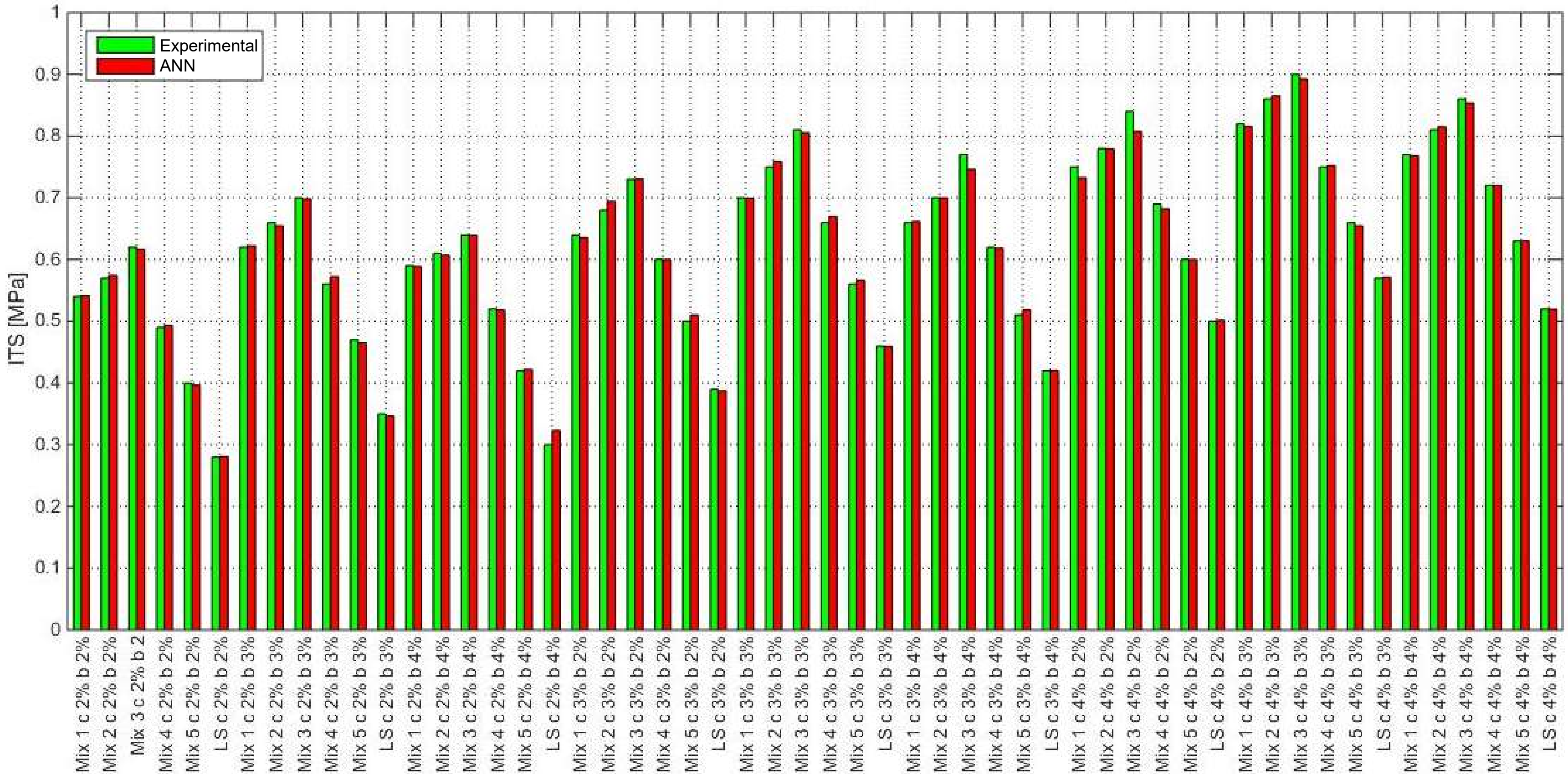

Wet ITS (ANN output vs Experimental data)

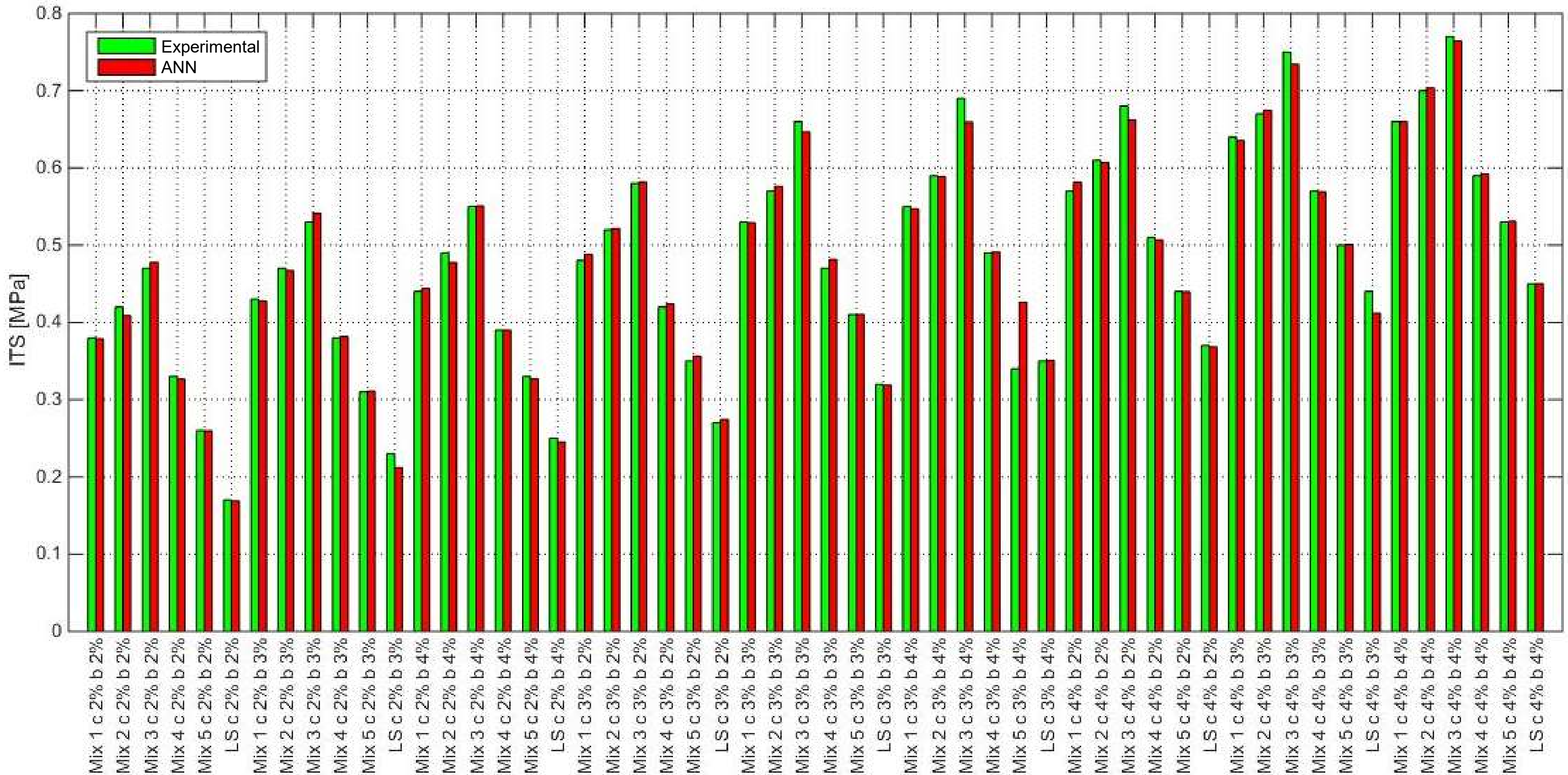

Stiffness (ANN output vs Experimental data)

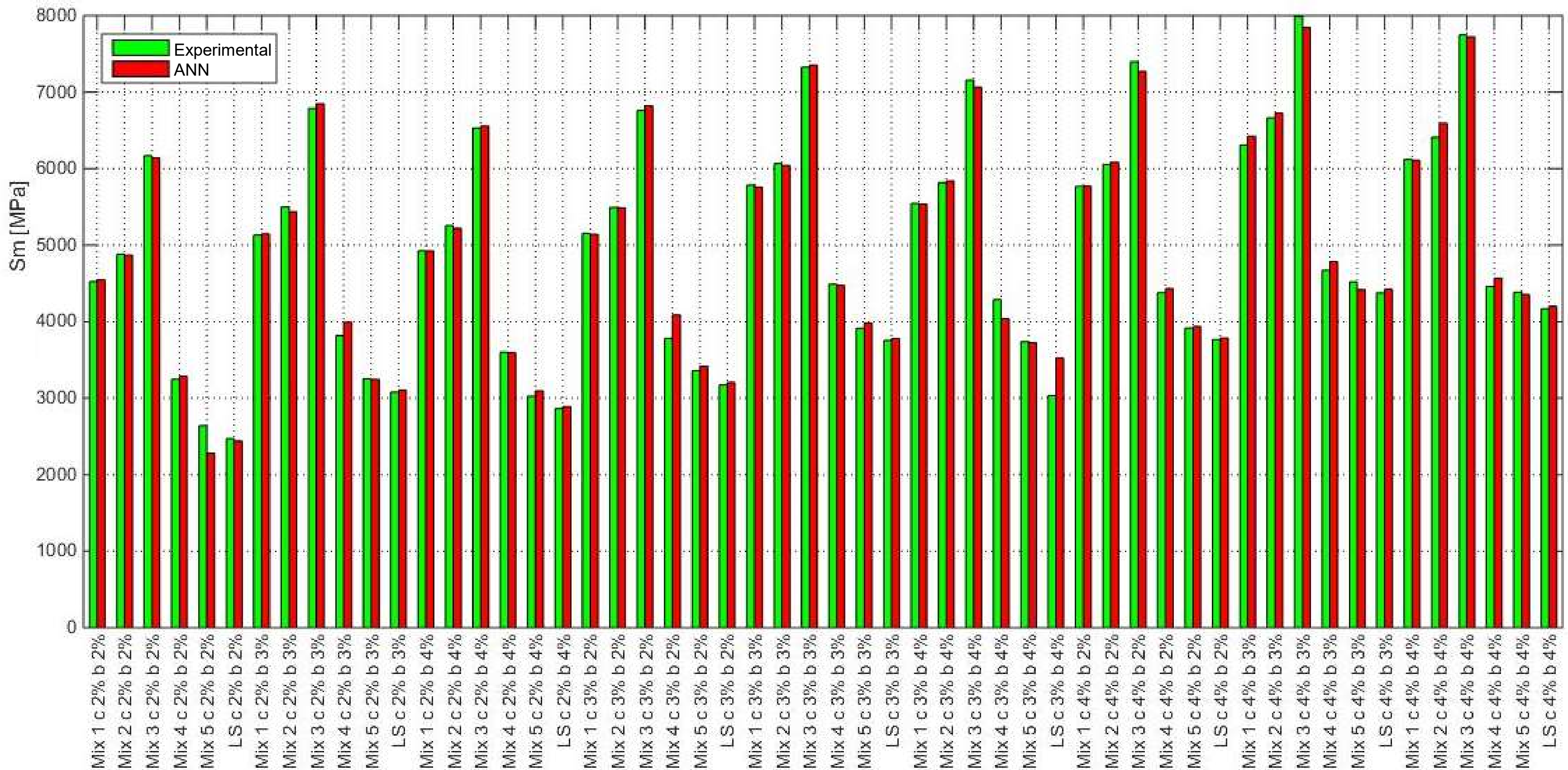

FINAL REMARKS (1/2)

1. Performance predictions via Machine Learning represent a contribution to ***Pavement Engineering Digitalization***.
2. Machine Learning non-linear fitting methods can positively contribute to the laboratory performance evaluation phase of bituminous mixtures, even for mixes with waste materials included in the composition, thus enforcing the *Green Transition* of Pavement Engineering.
3. Laboratory data consistency is a fundamental requisite to ensure neural models prediction accuracy.
4. Prediction accuracy is not based on the complexity of the model, but rather on the optimization of the model.

FINAL REMARKS (2/2)

1. SNNs (Shallow Neural Networks) have been shown to solve pretty well any multi-dimensional input-output fitting problem by providing an optimal number of hidden neurons.
2. The Bayesian optimization represents an effective approach to identify the optimal SNNs architecture and hyperparameters values.
3. The prediction accuracy of a SNNs model is very good, but a physical interpretation of the phenomena cannot be obtained (**BLACK BOX** issue).
4. Fatigue or permanent deformation resistance data should be included in the machine learning modeling, to further enhance the performance evaluation phase of asphalt concretes.

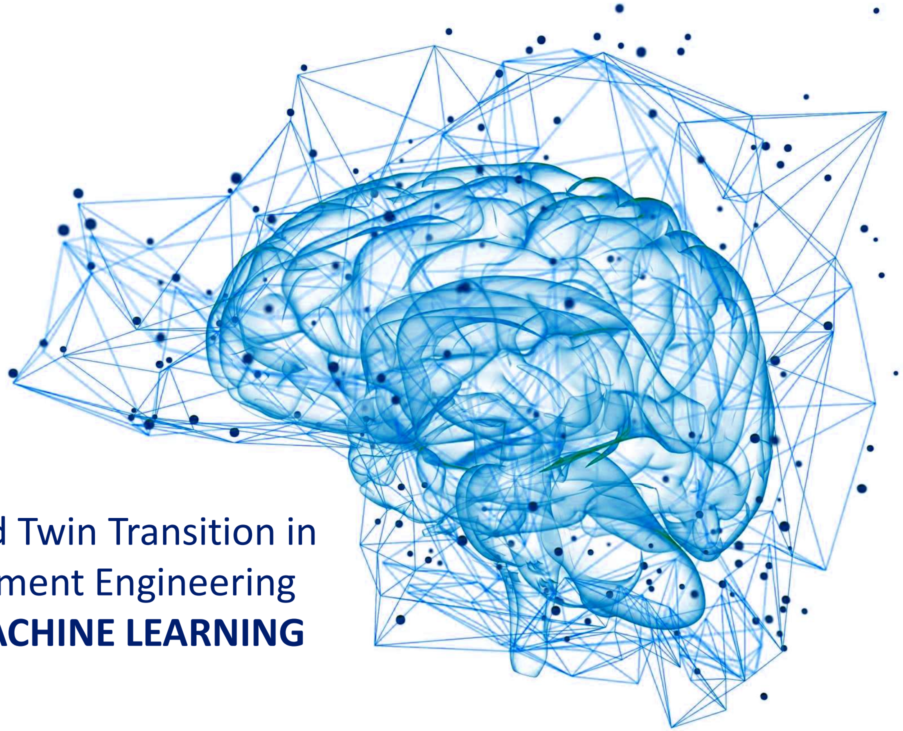

Toward Twin Transition in Pavement Engineering by **MACHINE LEARNING**

Università degli Studi di Perugia
Department of Civil and Environmental Engineering

Nicola Baldo
University of Udine

XIX International SIIV Summer School
Perugia 4th - 8th September 2023